Deliverable

D4.3: Catalogue for mapping geodiversity

Due date:	October 2020
Author:	Verner B. Ernstsen (UCPH/GEUS), Zyad Al-Hamdani (GEUS), Lars Ø. Hansen (GEUS), Mikkel S. Andersen (GEUS), Signe S. Hansen (UCPH), Aart Kroon (UCPH), Jørn Bo Jensen (GEUS)
Nature:	**RE**
Dissemination level:	**PP**

1 Introduction

Geodiversity is defined as "the natural range of geological, geomorphological, soil and hydrological features; and it includes their assemblages, structures, systems and contributions to landscapes" (Gray, 2013). The word and concept of "geodiversity" were first introduced in 1993 shortly after the Convention on Biological diversity was agreed at the UN Rio Earth Summit in 1992 (Gray, 2018). However, its recognition by a larger scientific audience and within society is still constraint by the lack of an established conceptual and methodological framework (Brilha et al., 2018).

The geodiversity concept has developed on land. Only recently, Gordon et al. (2016) carried out a study of large-scale seabed geodiversity around Scotland for assessing geoheritage, and Kaskela et al. (2017a) performed a basin-wide analysis of the Baltic Sea to assess geodiversity measures and patterns based on parameters like richness, patchiness and a geodiversity index. However, these studies were based on broad-scale datasets, neglecting multiple and small-scale geodiversity elements.

The overall scope of ECOMAP WP4 is remote sensing of geodiversity for habitat mapping, i.e. the focus of WP4 is on the abiotic elements of benthic habitats. The overall aim of WP4 is to develop the best-practice of combined hydroacoustic and optical mapping and monitoring of geodiversity and specific habitats at different water depths. The hydroacoustic being vessel borne multibeam echosounder (MBES) imaging and side scan sonar imaging, and the optical being airborne laser scanning (ALS) or Light Detection And Ranging (LiDAR).

More specifically, the main objectives of WP4 are 1) a feasibility study of LiDAR versus MBES for seabed classification, 2) morphometric analyses of larger scale areas, and 3) the development of a geodiversity catalogue and correlation of geodiversity with underlying geology, morphodynamics and hydrodynamics. The tasks within WP4 to achieve these objectives are T4.1 Repetitive opto-acoustic acquisition of stone reefs, sandbanks, and bubble reefs (M1-24), T4.2 Developing geological and geomorphological models (M19-M35), and T4.3 Developing best-practice for mapping and monitoring geodiversity (M25-36).

The above listed tasks lead to three deliverables within WP4: D4.1 Mapping of benthic flora with LiDAR and MBES (M24); D4.2 Geological and geomorphological models (M35); and D4.3 Catalogue for mapping geodiversity (M36).

This report comprises deliverable D4.3 on the development of a catalogue for mapping geodiversity. It combines work related to all three tasks: T4.1 Repetitive opto-acoustic acquisition of stone reefs, sandbanks, and bubble reefs, T4.2 Developing geological and geomorphological models, and T4.3 Developing best-practice for mapping and monitoring geodiversity. Moreover, the report includes previous work on the underlying geology at the selected test site.

The aim of the study presented in this report was to develop a catalogue for mapping geodiversity in coastal marine environments. The objectives were 1) to map the subsurface geology, the seabed sediments, the geomorphology, and the benthic habitats; and 2) to integrate the subsurface geology, seabed sediments and geomorphology in a seabed geodiversity index; 3) to relate the spatial distribution of seabed geodiversity to the spatial distribution of benthic habitats with a focus on specific habitats, including sandbanks, stone reefs and bubbling reefs.

The report briefly describes the selected test site and the applied materials and methods; it presents the subsurface geology, the seabed sediments, the geomorphology, the benthic habitats, and the geodiversity; it outlines some recommendations for future geodiversity mapping for improved habitat mapping; and it summarizes the findings with concluding remarks.

2 Selected test site

The selected test site presented in this report is the Hirsholmene marine habitat area off Frederikshavn in northern Denmark (see Figure 3). The selected test site displays multiple habitat types. In addition, existing data from previous surveys are available at this test site. This enables integration of existing data and results with the data acquired and the results generated in the ECOMAP project. The selected marine habitat test site is described below in terms of overall geological settings; water depth and bathymetry; sediment and substrate types; EU habitat types, broad-scale EUNIS habitat types and MSFD Benthic Broad Habitat Types as well as flora.

The overall geological settings in northern Denmark, where the Hirsholmene marine habitat area off Frederikshavn is located, are characterised by deeper faults, large Quaternary deposits, glacial deformation and deposition, and finally Holocene marine deposits.

Brandes et al. (2018) reviewed the tectonic settings in northern Denmark. The Tornquist Zone is a major lithospheric structure that extends from the Central North Sea across Denmark and the Baltic Sea into Poland. It is subdivided into a NW segment referred to as the Sorgenfrei-Tornquist Zone (STZ) and a SE part referred to as the Teisseyre-Tornquist Zone (TTZ). The STZ in northern Denmark is interpreted as a major tectonic structure that separates the Danish Basin from the Fennoscandian Shield and is considered to be a deep-seated fault zone. Based on interpretations of seismic sections on the northern flank of the STZ close to the Swedish coast, Gregersen et al. (1996) suggested that the deformation structures in the Quaternary sediments were the result of reactivation of the northern boundary fault of the STZ around the time of deglaciation. The findings of Gregersen et al. (1996) were further accentuated by results from sequence stratigraphy, biostratigraphy and 14C dating from the southern part of Kattegat, where deformed Lateglacial sediments associated with a NW-SE elongated depression were found (Jensen et al., 2002). Jensen et al. (2020) concluded that the deformations were caused by reactivation of faults in the Fennoscandian Border Zone because of the Late Weichselian isostatic adjustment. The southern and eastern parts of Kattegat covered by the two examples mentioned above are within the part of the STZ with the highest intensity of historic earthquakes in Denmark (Gregersen and Voss, 2012).

Larsen et al. (2009) reviewed the Pre-Quaternary surfaces and the large Quaternary deposits in northern Denmark. The area is part of the Kattegat Depression, a deep NW-SE trending basin that can be perceived as a SE branch of the Norwegian Channel (Lykke-Andersen et al. 1993). In northern Denmark, the pre-Quaternary surface descends towards the north from the present sea level or above to more than 250 m BSL. Hence, the thickness of Quaternary sediments in the most northern part of Denmark exceeds 250 m (Figure 1).

The combination of large Quaternary deposits, which contain biogenic deposits of the Eemian interglacial, with active faulting enables the release of biogenic gases in the seabed and also at the seabed surface and into the water column.

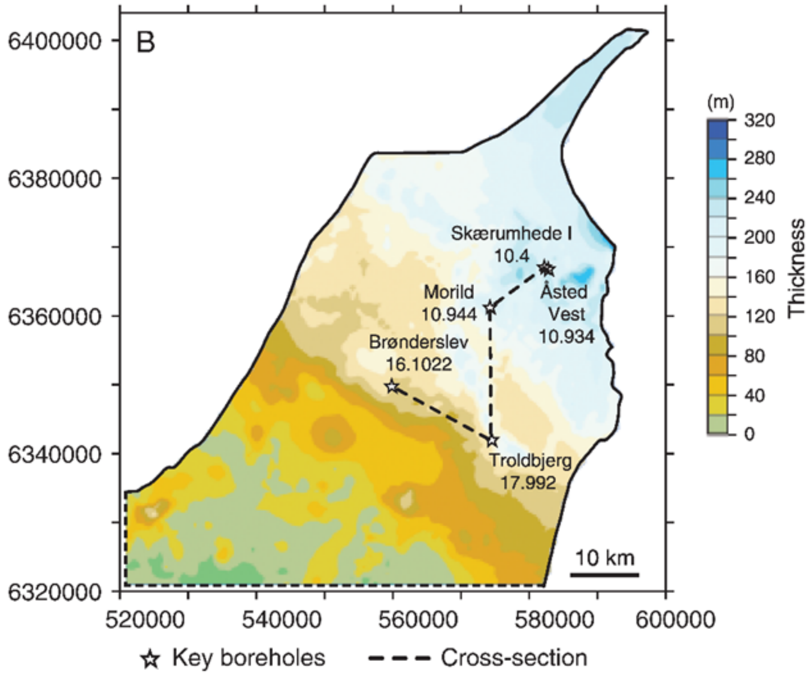

Figure 1. Thickness of the Quaternary sediments in northern Denmark (Fig. 2B in Larsen et al., 2009).

Krohn et al. (2009) reviewed the deglaciation after the Late Weichselian main advance in northern Denmark. Deglaciation towards the east with ice margins interpreted from location of buried valleys and topography as well as inferred hypothetical ice margins are shown in Figure 2 (Left), while the late glacial inundation of northern Denmark is shown in Figure 2 (Right). These paleogeographical reconstructions indicate ice margin deposits in the offshore Hirsholmene area off Frederikshavn.

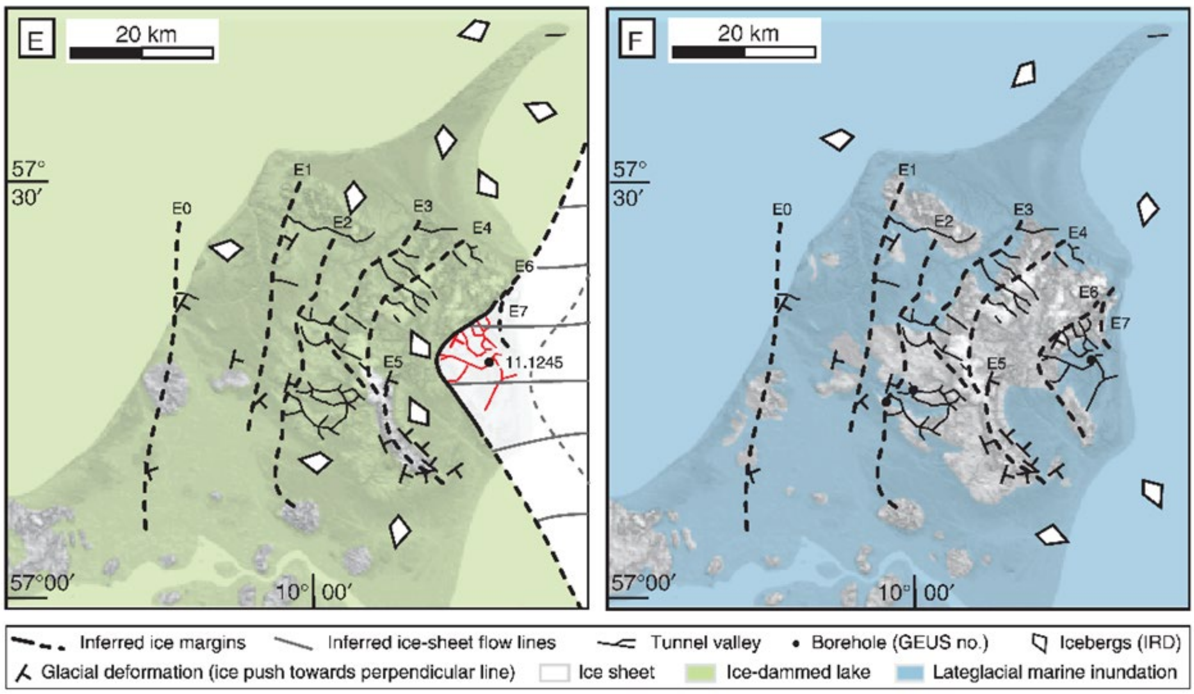

Figure 2. Paleogeographical reconstruction with ice margins and tunnel valleys from Sandersen et al. (2009). Left: Deglaciation towards the east, ice margin at the Sæby moraine, c. 19–18 kyr BP. Right: Lateglacial marine inundation, c. 18 kyr BP (Fig. 10E and F in Krohn et al., 2009).

The Hirsholmene marine habitat area off Frederikshavn is part of habitat area H4 “Hirsholmene, havet vest herfor og Ellinge Å’s udløb”, which is part of Natura 2000 area no. 4 with the same name (for location see Figure 3).

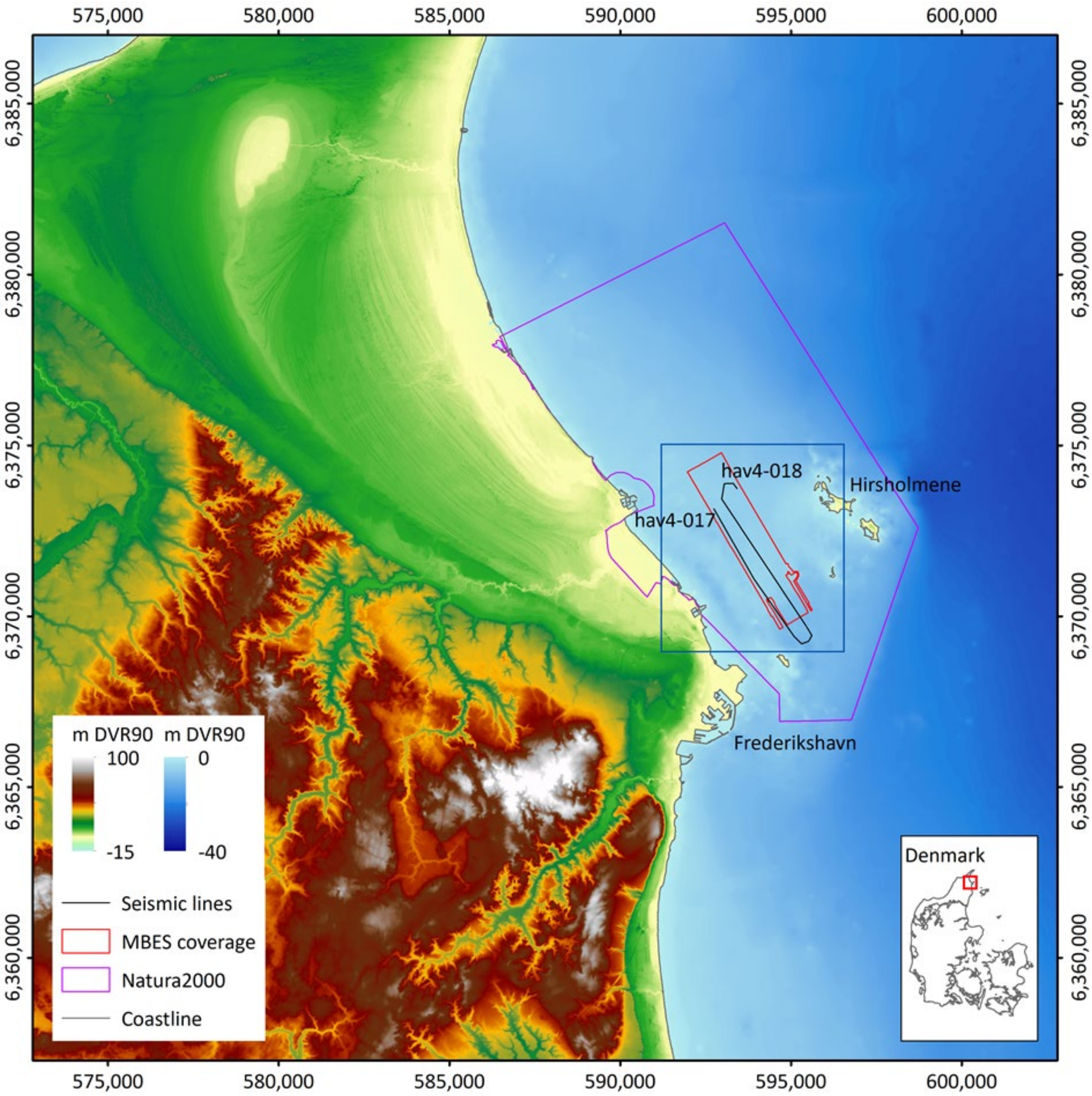

Figure 3. Test site Hirsholmene marine habitat area off Frederikshavn in northern Denmark. The background is the national DEMs of topography and bathymetry available from the Danish Geodata Agency. Projection is ETRS89 UTM Zone 32N with units in meter.

The water depths in the area are in the range 0-12 m. The area is generally shallow and flat, however with a marked depression parallel to the coastline as well as increasing water depths offshore the Hirsholmene islands.

The overall substrate types in the area are sand and mixed sediment (EMODnet Geology, 2019) based on the investigations of NST (2013). The mixed sediments are classified as till/diamicton according to the national Danish seabed sediment map (GEUS marine database MARTA). The earlier habitat mapping investigations comprised a combined analysis of satellite images, aerial orthophotos and

acoustical survey lines with single beam echosounding, side scan sonar imaging and sediment echosounding (sub-bottom profiling) as well as ROV video imaging for ground-truthing (NST, 2013).
The EU habitat types in the area are sandbanks (1110), reefs (here stone reefs) (1170) and submarine structures made by leaking gases (or bubbling reefs) (1180) (EMODnet Seabed Habitats, 2019) based on the investigations of NST (2013) (see Figure 4). Moreover, the area is classified as coastal lagoon (1150) and large shallow bay (1160) (NST, 2013).

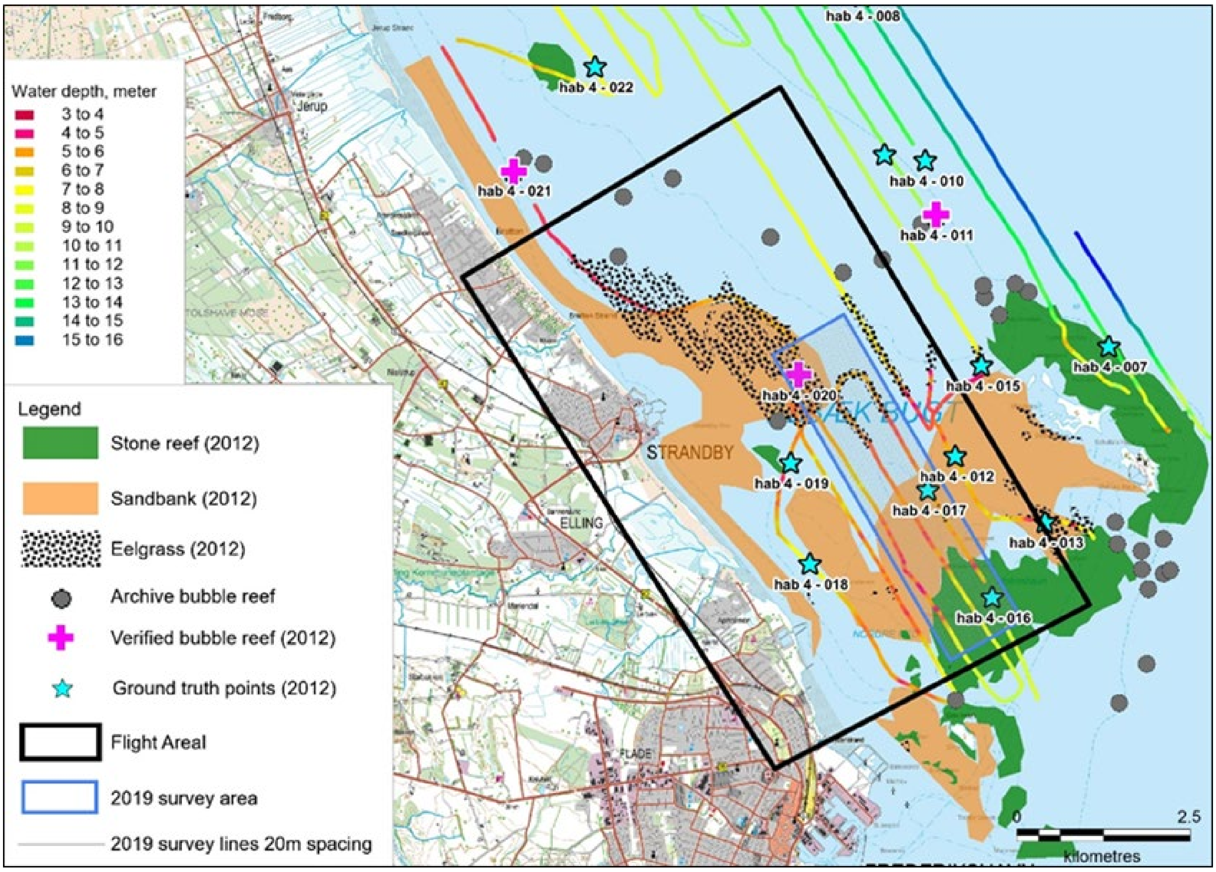

Figure 4. Test site Hirsholmene marine habitat area off Frederikshavn in northern Denmark with EU habitat types and coverage of LiDAR surveys and MBES survey carried out in 2019.

The EUNIS habitat types in the area are infralittoral fine sand or infralittoral muddy sand (A5.23 or A5.24), circalittoral fine sand or circalittoral muddy sand (A5.25 or A5.26), infralittoral mixed sediments (A.5.43) and circalittoral mixed sediments (A5.44) (EUSeaMap, 2019; EMODnet Seabed Habitats, 2019). The corresponding MSFD Benthic Broad Habitat Types are infralittoral sand, circalittoral sand, infralittoral mixed sediment and circalittoral mixed sediment. The difference between EUNIS habitat types and MSFD Benthic Broad Habitat Types is that the latter are consistent between basins, whilst the EUNIS habitat types are region-specific and potentially more detailed than the MSFD Benthic Broad Habitat Types, owing to the specific conditions relevant to each region (EMODnet Seabed Habitats, 2019). In case of the Hirsholmene area, the spatial delineation of the EUNIS habitat types and the MSFD Benthic Broad Habitat Types is identical, and it follows the spatial distribution of substrate types.
The dominating flora in the stone reef areas, corresponding to the areas with mixed sediment substrate, is brown and red algae communities (NST, 2013). On the sandy substrate, the dominating benthic flora is common eelgrass (*Zostera marina*) (NST, 2013). The Hirsholmene islands form the top of one of the largest coherent stone reefs in Danish waters (NST, 2013). Hence, the Hirsholmene

marine area is an ideal natural laboratory for developing new methods for improved habitat mapping in shallow coastal waters.

3 Materials and methods

The subsurface geology at the test site was analysed on the bases of archive sub-bottom profiler data acquired in earlier studies.
The geomorphology and benthic habitats were mapped using MBES and LiDAR (in combination with video imaging for ground truth) during the ECOMAP project as part of task T4.1 Repetitive opto-acoustic acquisition of stone reefs, sandbanks, and bubble reefs (M1-24).
The surveys and instrumental setups are described below, along with a brief outline of the data processing and the data analyses.

3.1 Archive subsurface geology

Sub-bottom profiler (SBP) data were acquired by GEUS in the Hirsholmene marine habitat area off Frederikshavn in a previous study (19-20 August 2012) (NST, 2013). The SBP data were recorded using an Innomar SES-2000 Standard SBP. The high ping rate, small footprint and the possibility of transmitting sound pulses over a wide frequency range ensure sub-seafloor data with high resolution in the order of 0.05 m.
The SBP data were processed in the software Geosuite. Proprietary filters like frequency filters and automatic gain settings were applied to the data, and wave noise was reduced by swell filtering. Subsequently, the SBP data were exported to Kingdom Suite which was used for the data analysis. The interfaces between facies with different densities were identified semi-automatically by following the amplitude of the seismic signals and seismic units.

3.2 Seabed sediments, geomorphology and benthic habitats

3.2.1 Surveys and instrumental setup

One MBES dataset and two LiDAR datasets were acquired in the Hirsholmene marine habitat area as part of task T4.1 Repetitive opto-acoustic acquisition of stone reefs, sandbanks, and bubble reefs (M1-24).

The MBES dataset was collected by GEUS during a midsummer survey in the blooming season (within the period 11-19 June 2019), i.e. the midsummer 2019 LiDAR and MBES surveys were carried out with only a few days in between. During this period (17-19 June 2019), UPCH/GEUS also collected ground truth data in terms of seabed samples as well as pictures and video of the seabed from diving.
The EdgeTech 6205 dual frequency side scan (230 & 550 kHz)/swath bathymetry (550 kHz) system was applied. This is a Multi Phase Echo Sounder (MPES) system; however, we refer to it as MBES in this context. The swath width for the side scan was set to 50 m. This ensured high-resolution seabed images that enhance interpretation of seabed sediments and habitats. The system was bow-mounted on the GEUS survey boat "Maritina" to ensure minimum interference and noise. The Applanix POS MV was used for providing navigation and attitude data and RTK GPS was used for the positioning.

The LiDAR datasets were collected by Airborne Hydro Mapping GmbH (AHM) during two separate surveys: a spring survey in the beginning of the blooming season (17 April 2019) and a midsummer survey in the blooming season (21 June 2019).

A twin-engine plane (Tecnam P2006T) was used as flight deck with a laser scanner (RIEGL VQ-880-G) integrated in the frontal part of the aircraft. The laser scanner emits a green laser pulse with a wavelength of 532 nm with a laser pulse repetition rate of up to 550 kHz. The flight altitude was 400 m, which combined with a laser beam divergence of 1.1 mrad, yields a laser beam footprint of ~0.4 m. The laser scan pattern is circular with an incidence angle of 20°, generating a scan pattern of curved parallel lines with a swath width of ~400 m at a flight altitude of 400 m. The point density is ~20 points/m^2 at a flight altitude of 400 m and a flight speed of ~80 kn (~150 km/h). According to RIEGL, the typical water depth measuring range is 1.5 Secchi depth. The laser scanner system records full waveform data. Intensity information is provided for each returned signal.
Aerial RGB images were recorded by an aerial camera (Hasselblad H3D-39 with a focal length of 35 mm) integrated in the back of the aircraft. The ground sampling distance (GSD) of the RGB images is ~8 cm at a flight altitude of 400 m. The RGB images serve also as ground truth data due to this high image resolution.
Aircraft position and attitude was recorded by a GNSS/IMU navigation system at a rate of 256 Hz consisting of a compact GNSS antenna (NovAtel 42G1215A-XT-1-1-CERT) mounted outside of the aircraft and an IMU (IGI AEROcontrol-IIe) mounted on top of the laser scanner.

3.2.2 Data processing

The MBES data were pre-processed (i.e. integrated and corrected) and post-processed (i.e. edited and filtered). The pre- and post-processing were performed using the dedicated software Qimera by QPS. The processing pipeline contained the overall steps of converting GPS heights to DVR90 using the Geoid02 model; correcting delayed heave using PosMV delayed heave; ray tracing using sonar head time series sound velocity (sound velocity profiles were measured during the survey period, showing a well-mixed water column with little to no vertical variation in sound velocity through the water column); patch testing for optimizing the sensor integration; automatic filtering of the soundings using a pre-defined medium spline filter – approximation of IHO Special Order; and exporting point-cloud soundings for gridding in ArcGIS. The filtered point-cloud soundings were gridded with a grid cell size of 1 m to generate a bathymetric map.
The SS part of the data was processed and interpreted with the SonarWiz 7 software. Both low frequency and high frequency channels were used in the interpretation whenever required. The 25 m swath side scan yields high-resolution data which was very useful in delineating small objects on the seabed. Each survey line was inspected in the SonarWiz software and different options were used (Automatic Gain Control AGC, and User define gain UGC/Attenuation control) as well as other processing tools were used to get the best image of the seabed.

The processing of the raw LiDAR data for producing a point cloud and subsequently a digital elevation model (DEM) followed the processing procedure outlined by Andersen et al. (2017). The processing pipeline contained the overall steps of determining the flight trajectory; georeferencing the point cloud; aligning the swaths (i.e. strip adjustment) to minimize the bias between individual swaths; filtering (or classifying) the point cloud to remove noise; detecting the water surface (i.e. water surface modelling); correcting all points below the water surface for refraction of the laser beam; and producing a DEM from the filtered and corrected point cloud (see Andersen et al. (2017) for a detailed description of each step). The processing pipeline, specifically the filtering/classification step and the water surface modelling step, has been further developed and optimised within the ECOMAP project in order to improve the quality of the filtering/classification and to reduce the processing time, which is essential when working with large datasets (i.e. millions of points with multiple attributes).

3.2.3 Data analysis and classification

Seabed sediments

The seabed sediment interpretation was based on the side scan imagery in combination with ground truth data as well as previous knowledge of the area available from the GEUS MARTA database and particularly from the 2012 habitat mapping of the area (NST, 2013) as shown in Figure 4.

Geomorphology

The analysis and classification procedure for generating the geomorphological map was a two-step procedure. Initially, a geomorphometric classification analysis was made using the ArcGIS extension Benthic Terrain Modeler (BTM) (Walbridge et al., 2018), developed by Wright et al. (2005). Subsequently, an expert geomorphological classification was performed based on the seabed sediment and geomorphometric analyses. See also Andersen et al. (2017) and Hansen et al. (submitted) for further details on applying a geomophometric classification analysis for geomorphological mapping.

Benthic habitats

Benthic habitats were designated based on the seabed sediment, geomorphometric and geomorphological analyses in combination with ground truth data, i.e. video imaging data acquired during the ECOMAP project and archive data.

3.3 Seabed geodiversity

3.3.1 Geodiversity index

Building a seabed geodiversity index of the test area involved a scale analysis to determine appropriate scale levels of the input parameters used in the computation of the geodiversity index. The input parameters included geomorphometric structures, seabed sediments and a measure of surface roughness. The Geodiversity Index was calculated as:

$$GD=EG\ R/\ln S$$

where GD is Geodiversity Index, EG is the number of elements in the unit, R is the roughness of the unit, ln is the natural logarithm, and S is the unit surface area (Serrano and Ruiz-Flaño, 2007).
We applied a slightly adapted version of the approach presented by Kaskela and Kotilainen (2017). We derived EG from the morphometric classification and the seabed substrate layers, while Kaskela and Kotilainen (2017) also included subsurface geology. The roughness R is defined as the standard deviation of the slope within the unit area.
The resulting Geodiversity index was classified according to quartiles where the 1st quartile is the lowest geodiversity and the 4th quartile is the highest geodiversity (Kaskela and Kotilainen, 2017).

We constructed the geodiversity index on two selected scale levels: the highest resolution (1 m grid cell size) and a grid cell size derived from the scale level analysis as the first significant peak (cf. section on scale analysis below).

Scale analysis

The scale analysis (after Drăgut et al. 2010 and 2011) was performed to determine appropriate scale levels of the analysis. Drăgut et al. (2010 and 2011) adopted the method from Woodcock and Strahler (1987) who developed a method of data-driven scale-detection for image analysis. The method uses Local Variance (LV) as a measure for spatial structure, which is primarily related to spatial resolution and size of objects in the image (Woodcock and Strahler, 1987).

The scale analysis approach computes LV as the standard deviation of slope within a 3 x 3 grid cell window. Each grid cell of the surface model is thus assigned a value of LV and the mean value of the entire surface is then taken as LV at that specific scale level, i.e. grid cell resolution (Woodcock and Strahler, 1987; Drăgut et al. 2010 and 2011). LV is computed at multiple scales by successively degrading the raster resolution (Drăgut et al. 2010 and 2011). The method builds on the principle of spatial autocorrelation in the sense that most cells are highly correlated with their neighbours when raster cells are considerably smaller than features on the DEM, resulting in low LV. LV begins to increase when the raster grid cell size begins to approximate the size of features in the DEM (Drăgut et al. 2011). The Rate of Change of Local Variance (ROC-LV) enables multi-scale analysis by measuring the dynamics of LV from one scale level to the next (Drăgut et al. 2010).

The scale analysis was conducted on both elevation and slope derived from the Hirsholmene bathymetry. The investigated range of scale levels spanned from 1 m to 20 m grid cell size.

The first significant peak was observed at a grid cell size resolution of 11m with respect to both elevation and slope (Figure 5).

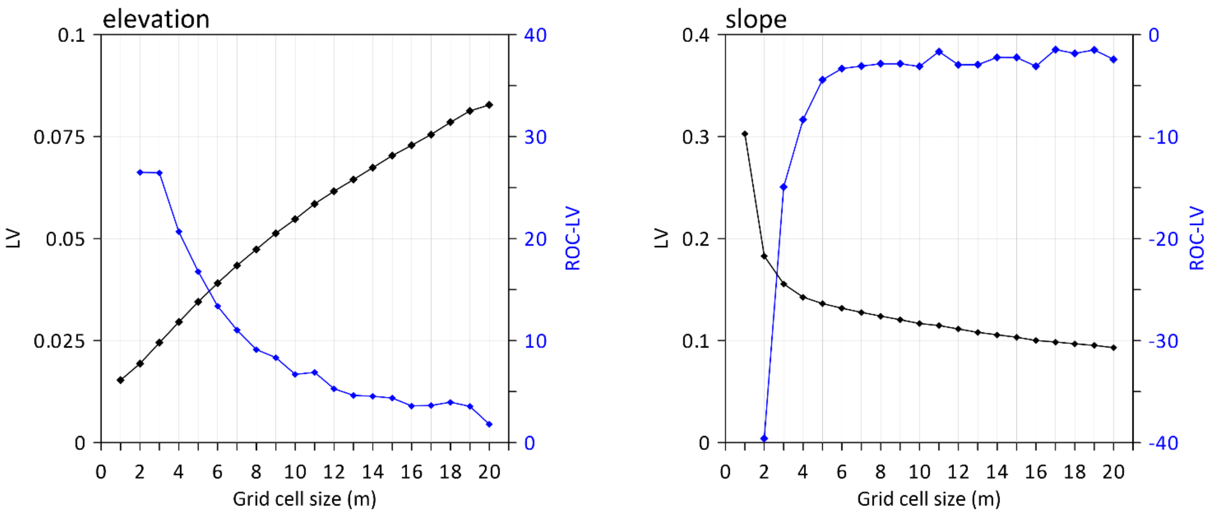

Figure 5. Scale analysis on elevation (left) and slope (right) for the test site Hirsholmene marine habitat area off Frederikshavn in northern Denmark derived from bathymetry.

Geomorphometric classification analysis (EG input)

The geomorphometric classification analysis was the most detailed input to the Geodiversity computation as it was derived from the DEM.

The classification was done with the Benthic Terrain Modeler (BTM) developed by Wright et al. (2005). The analysis applies Bathymetric Position Indices (Wright et al., 2005) modified from Weiss' (2001) Topographic Position Index. Broad-scale BPI (B-BPI), Fine-scale BPI (F-BPI), slope, and a classification dictionary are the required inputs to the BTM.

A broad-scale BPI (B-BPI) was computed from focal statistics with an annulus radius of 100 m (100 grid cells) and 99 m (9 grid cells) for the 1m resolution and 11m resolution, respectively. A Fine-scale BPI (F-BPI) was computed with an annulus radius of 19 m (19 grid cells) and 22 m (2 grid cells), respectively.

The 100 m radius was selected as it corresponds to the approximate trough-to-trough distance of the large bedforms just northwest of the stone reef area. The 19 m scale factor corresponds to a secondary peak observed in the scale analysis (see Figure 5).

The BPI computations were done on a z-exaggerated (5x) DEM to capture a higher level of detail of the complex bathymetry observed in the area. BPIs were standardized prior to the BTM classification so that BPI mean is zero and one standard deviation is equivalent to +/- 100 BPI (Weiss, 2001).

Resulting BPIs and slope were used as input to the BTM classification. A classification dictionary designating 12 geomorphometric classes was built for the purpose. It was decided to set class boundaries at +/- 50 BPI. Similar class boundaries were applied by e.g. Kaskela et al. (2012) and Andersen et al. (2017), while Hansen et al. (submitted) applied boundaries of +/- 100 BPI in relation to low-topography washover fans in the coastal zone. Slope thresholds differentiating flat areas from sloping ones were determined for each grid cell resolution as the mean plus one standard deviation of each slope surface (see Table 1). The slope thresholds were 1.7° and 0.7° for the 1 m and 11 m grid cell resolution.

Table 1. Geomorphometric classification dictionary. BPI Lower and Upper columns define standardized BPI class boundaries. A BPI of +/- 50 corresponds to a standard deviation of +/- 0.5. Slope delimiter value is defined as slope mean + 1 std of the specific slope surface in terms of grid cell size. Slope values displayed in the table were used with the 1 m grid cell size classification.

Class	Zone	B-BPI Lower	B-BPI Upper	F-BPI Lower	F-BPI Upper	Slope Lower	Slope Upper
1	Small scale depression		-50		-50		
2	Depression		-50	-50	50		
3	Small scale crest in depression		-50	50			
4	Small scale depression on flat	-50	50		-50		1.7
5	Small scale depression on slope	-50	50		-50	1.7	
6	Flat	-50	50	-50	50		1.7
7	Slope	-50	50	-50	50	1.7	
8	Small scale crest on flat	-50	50	50			1.7
9	Small scale crest on slope	-50	50	50		1.7	
10	Small scale depression on crest	50			-50		
11	Crest	50		-50	50		
12	Small scale crest	50		50			

Seabed sediments (EG input)

The seabed sediment layer was derived from expert interpretation of side scan sonar data. The layer was resampled to align to the sizes of the other raster layers, i.e. 1 m and 11 m grid cell sizes.

Physical elements of EG

The EG input of the Geodiversity index consists here of the geomorphometry and seabed sediment classes. Patch richness was taken as the measure of EG. Patch richness is the variability of patches (i.e. the number of different classes) within a predefined neighbourhood (Kaskela and Kotilainen, 2017). The patch richness was quantified using ArcGIS Focal statistics tool with a disk-shaped neighbourhood having a radius of 55 m; this is equivalent to an area of 9,503 m^2, which is the unit area S in the Geodiversity index equation. The 55 m radius was chosen in order to capture what appears to be the largest scale of interest (i.e. trough-to-trough distance of ca 100 m of the large bedforms) and to ensure similar size of the analysis area with both 1 m and 11 m grid cell size (i.e. 55 cells and 5 cells radii).The resulting patch richness of the geomorphometry and the seabed sediment layers were then summed to give the total variability (i.e. the EG layer) of each grid cell in relation to the investigated neighbourhood.

Seabed roughness (R)

Seabed roughness was computed from ArcGIS Focal statistics tool as the standard deviation of slope within a predefined disk-shaped neighbourhood (Kaskela and Kotilainen, 2017). The roughness was computed with a neighbourhood radius of 55 m as in case of the physical elements (EG).

4 Results

4.1 Subsurface geology

The two SBP lines at Hirsholmene oriented NW to SE are shown in Figure 6 with the eastern profile as the upper and the western profile as the lower. The SBP data reveal a density interface that is generally buried in the NW part while being exposed in the SE part. The interface is interpreted as the surface of glacial moraine deposits. The overlying facies in the NW part and in isolated places in the SE part is interpreted as Holocene marine sand deposits. The exposed glacial moraine deposits are confirmed as hard ground from video ground truth; and likewise, the sand deposits are also confirmed from video ground truth and seabed sampling (the grain size analysis are still ongoing as mentioned above).
The most western SBP line reveals a depression in the seafloor associated with indications of gas in the SBP data. The depression is interpreted as an erosional feature, with the local erosion being due to higher erodibility due to a release of gas to the upper sand deposit from deeper biogenic deposits.

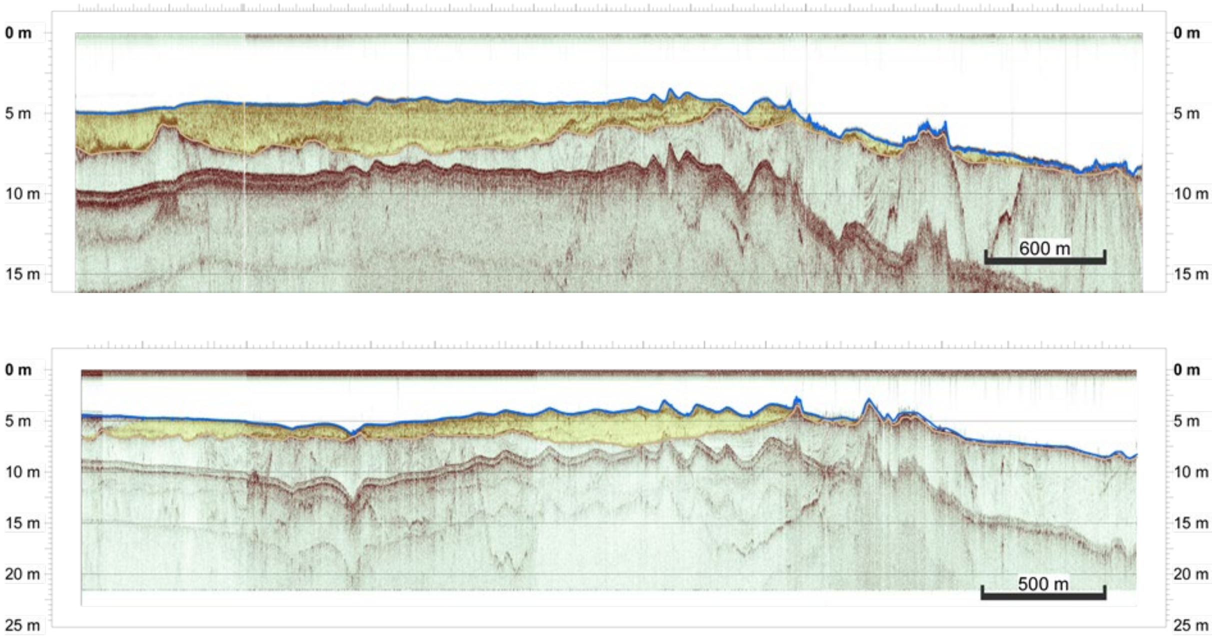

Figure 6. Sub-bottom profiler (SBP) data acquired by GEUS in the Hirsholmene marine habitat area off Frederikshavn in a previous study (19-20 August 2012) (NST, 2013).Upper: SBP-line hav4-018 from NW to SE; Lower: SBP-line hav4-017 from NW to SE (for locations see e.g. Figure 3 and Figure 8). Blue line marks the interpreted surface of the seafloor; Beige line marks the interpreted surface of the glacial moraine deposits, Yellow marks the interpreted Holocene marine sand deposits.

4.2 Seabed sediments

The seabed sediment map of the test site in the Hirsholmene marine habitat area off Frederikshavn is shown in Figure 7. The seabed sediment classes are Till, Sand, Coarse grain sediment, and Carbonate-cemented sandstone.

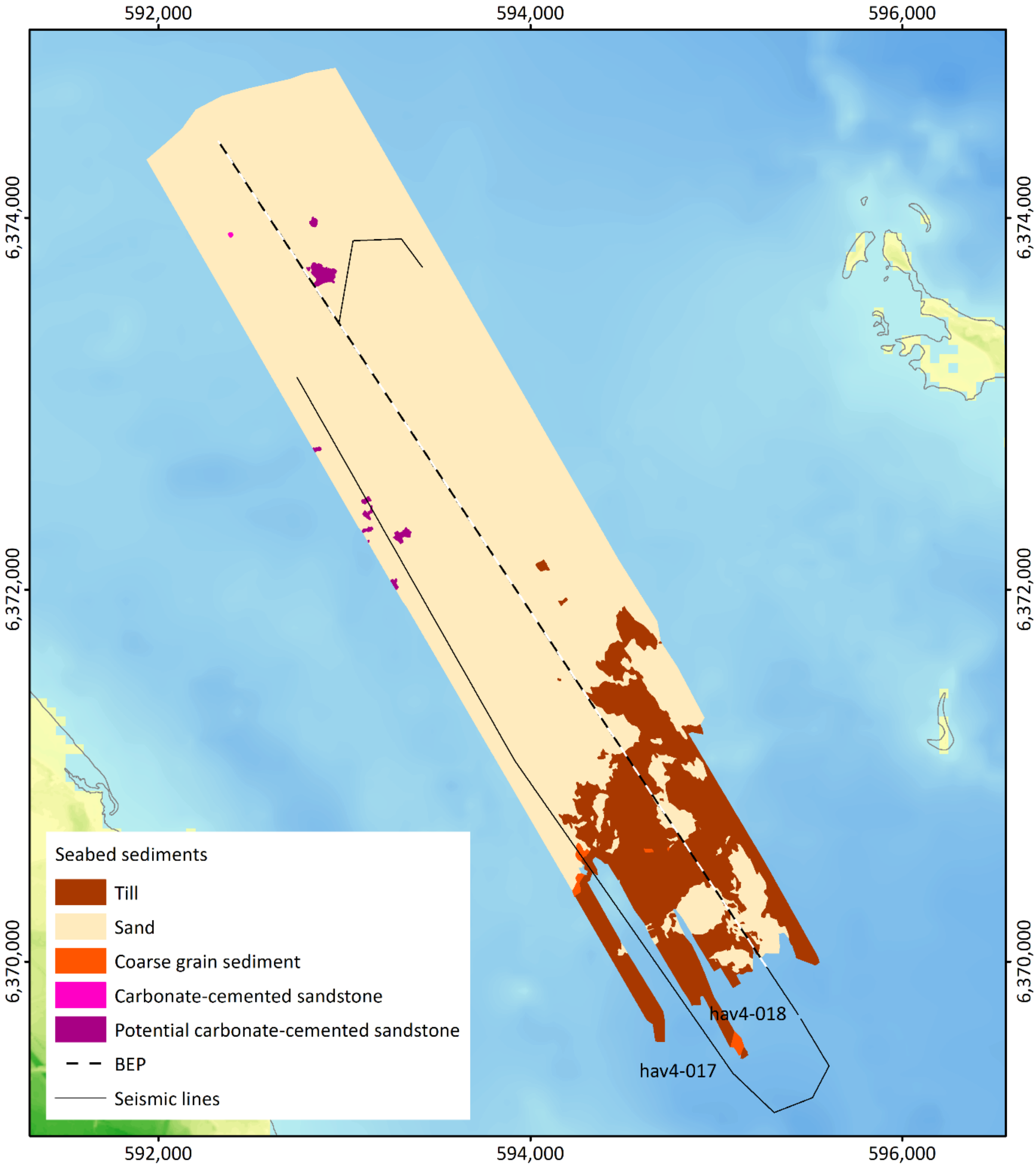

Figure 7. Seabed sediment map of the test site in the Hirsholmene marine habitat area off Frederikshavn derived side scan sonar data in combination with ground truth data (for location see Figure 3). The background is the national DEMs of topography and bathymetry available from the Danish Geodata Agency. Projection is ETRS89 UTM Zone 32N with units in meter.

4.3 Geomorphology

The bathymetry of the test site in the Hirsholmene marine habitat area off Frederikshavn is shown in Figure 8 with a grid cell size of 1 m. The water depths range from around 2 m to around 10 m with the deepest water depths in the SE part and the shallowest depths above the crests of the large bedforms in the central part. The bathymetry is the input for the geomorphometric analysis.

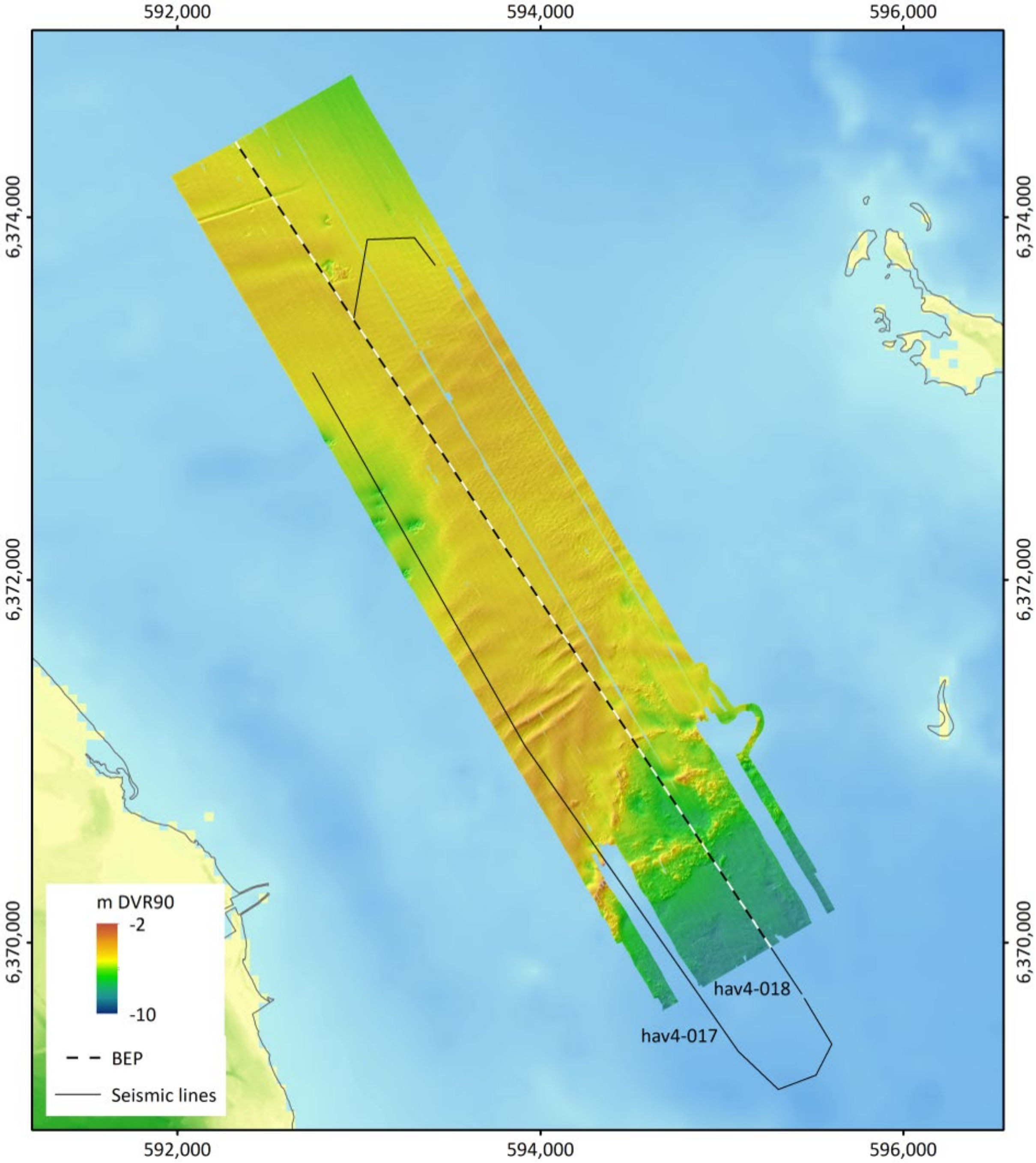

Figure 8. Bathymetry of the test site in the Hirsholmene marine habitat area off Frederikshavn derived from vessel borne MBES data (for location see Figure 3). The digital elevation model (DEM) is shown with a grid cell size of 1 m. The background is the national DEMs of topography and bathymetry available from the Danish Geodata Agency. Projection is ETRS89 UTM Zone 32N with units in meter.

The results of the geomorphometric BTM classification analysis are shown in Figure 9. The results are generalised in order to highlight the characteristics of the study site. The geomorphometric analysis reveals the generally flat areas in the northern half of the test site as well as the crests, troughs (depressions) and slopes of the bedforms in this area. In addition, it reveals the diverse and rugged areas towards the south with a mosaic of crests, slopes and depressions. Finally, the analysis identifies crests with an oblique orientation to the bedforms at the border between the generally flat areas towards the north and the more diverse and rugged areas to the south.

The bathymetric map, the geomorphometric BTM classification analysis along with other DEM derivatives are used for generating the geomorphological map of the test site.

Figure 9. Geomorphometric classification of the test site in the Hirsholmene marine habitat area off Frederikshavn (for location see Figure 3). The background is the national DEMs of topography and bathymetry available from the Danish Geodata Agency. Projection is ETRS89 UTM Zone 32N with units in meter.

The geomorphological map of the test site in the Hirsholmene marine habitat area off Frederikshavn is shown in Figure 10. The generally flat and sandy areas in the northern part of the test site with bedforms are classified as sandy mobile bedforms. The flat areas also display depressions with rugged outcrops, and in the most northern part a well-defined mound structure. The diverse and rugged areas towards the south are classified as outcrops with ground truth data showing that these areas display a gravelly hard substrate. This coincides with the reflector interpreted as the exposed glacial surface from the SBP data (cf. Figure 6). The crests with an oblique orientation to the bedforms at the border between the generally flat areas towards the north and the more diverse and rugged areas to the south are classified as ridge and swale structures, which is also the case in the most NW part of the test site. The flat areas in between the outcrops are classified as sandy mobile flats. This coincides with the deposits interpreted as sand from the SBP data (cf. Figure 6). Finally, the marked straight depression in the most northern part of the test site is a dredged navigation channel.

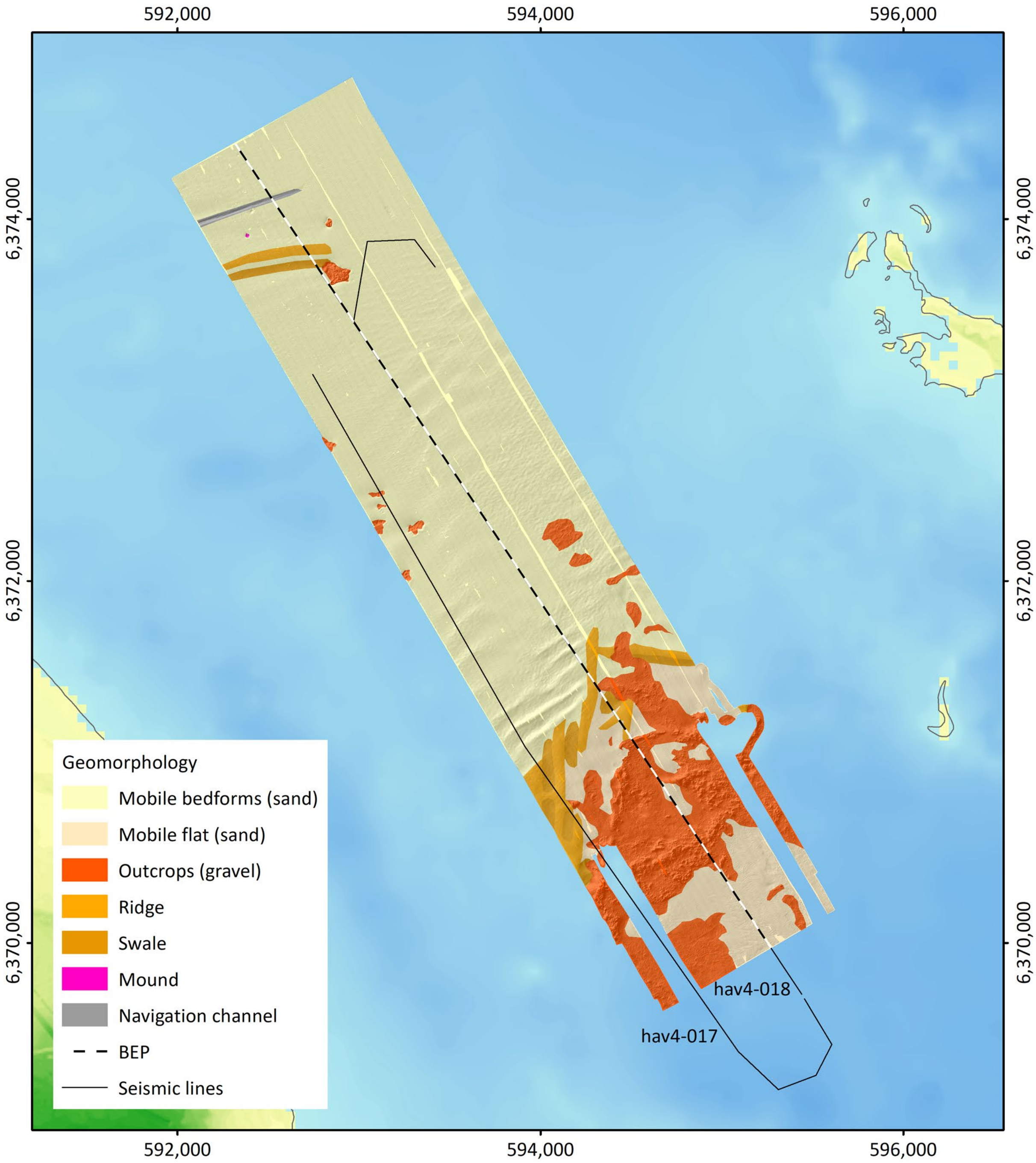

Figure 10. Geomorphological map of the test site in the Hirsholmene marine habitat area off Frederikshavn based on the geomorphometric classification (for location see Figure 3). The background is the national DEMs of topography and bathymetry available from the Danish Geodata Agency. Projection is ETRS89 UTM Zone 32N with units in meter.

4.4 Benthic habitats

The benthic habitat map of the test site in the Hirsholmene marine habitat area off Frederikshavn is shown in Figure 11. The habitat classification and the extent of the habitats is based on combining the subsurface geology and the geomorphology in combination with information from new and archive ground truth data. The major part of the sandy mobile bedforms area in the geomorphological map is classified as sandbank habitat area, including the ridge and swale areas. The depressions on the sand areas with rugged outcrop are classified as bubbling reef, including the well-defined mound in the north. The mound is known to be a bubbling reef from previous surveys, while the remaining depressions containing rugged features may be considered as potential bubbling reefs. The outcrops towards the south, which are interpreted as exposed glacial moraine deposits, are hard substrates classified as stone reefs.

The seagrass habitat is overlain from a previous study (NST, 2013). However, seagrass was also observed in the northern part on the sandy flats during the ground truth survey within the ECOMAP project.

The descriptive habitat names are similar to those of the EU Nature2000 Habitat Types; however, the habitat map is not to be considered as a Nature2000 habitat map. E.g. ground truth validation of the potential bubbling reefs is required, and likewise the stone density in the outcrop area must be estimated/determined in order to clarify the exact extent of the reef structure.

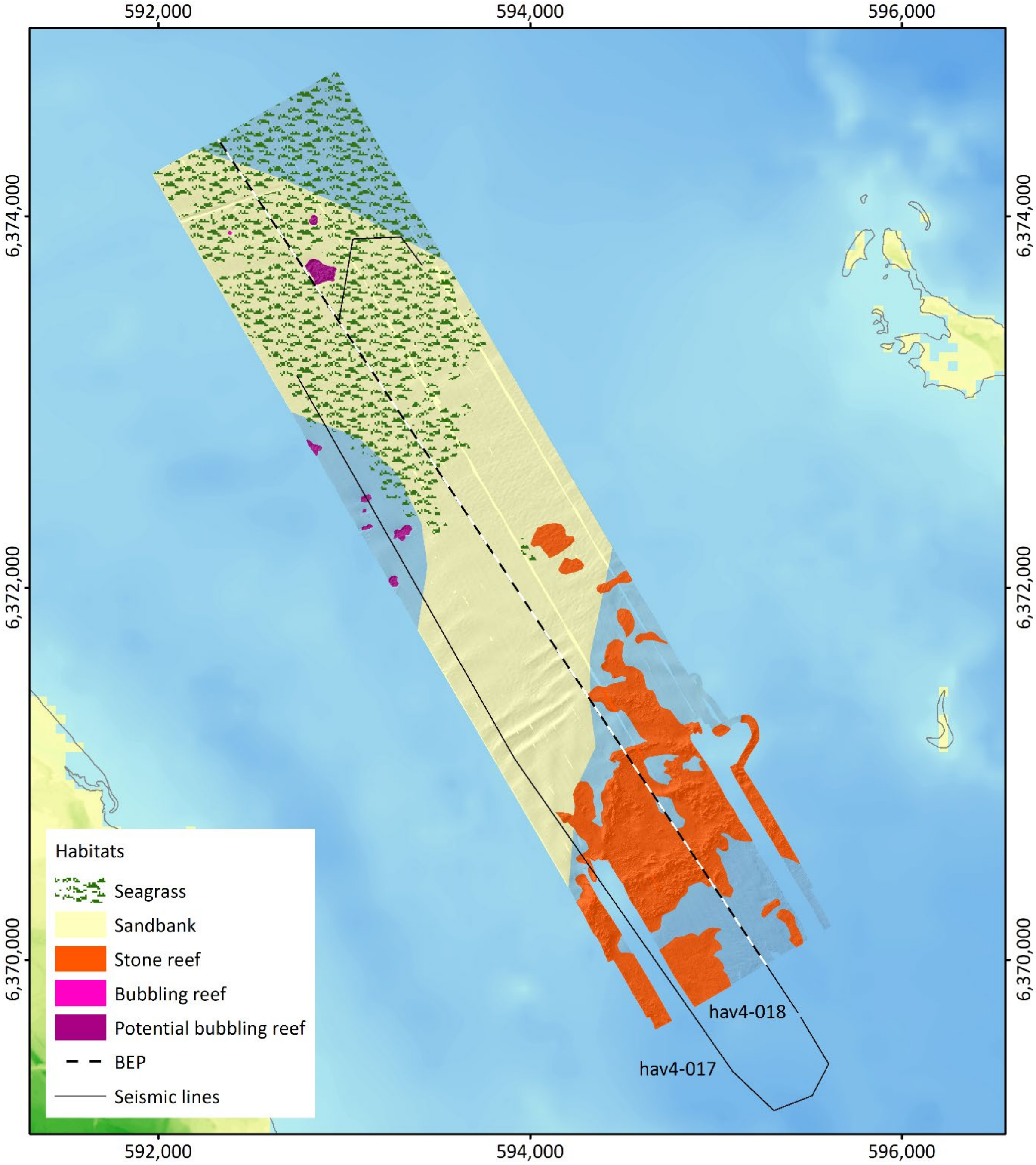

Figure 11. Benthic habitat map at the test site in the Hirsholmene marine habitat area off Frederikshavn (for location see Figure 3). The background is the national DEMs of topography and bathymetry available from the Danish Geodata Agency. Projection is ETRS89 UTM Zone 32N with units in meter.

4.5 Seabed geodiversity

The geodiversity index was computed from the seabed sediments and the geomorphometric features (EG-parameter in the geodiversity index) together with the surface roughness (R-parameter in the geodiversity index) (see equation in section 3.3.1 on the geodiversity index). The seabed sediment maps of the test site in the Hirsholmene marine habitat area off Frederikshavn adapted to grid cell sizes of 1 m and 11 m are shown in Figure 12 and Figure 13, respectively; i.e. these are identical to the seabed sediment map in Figure 7.

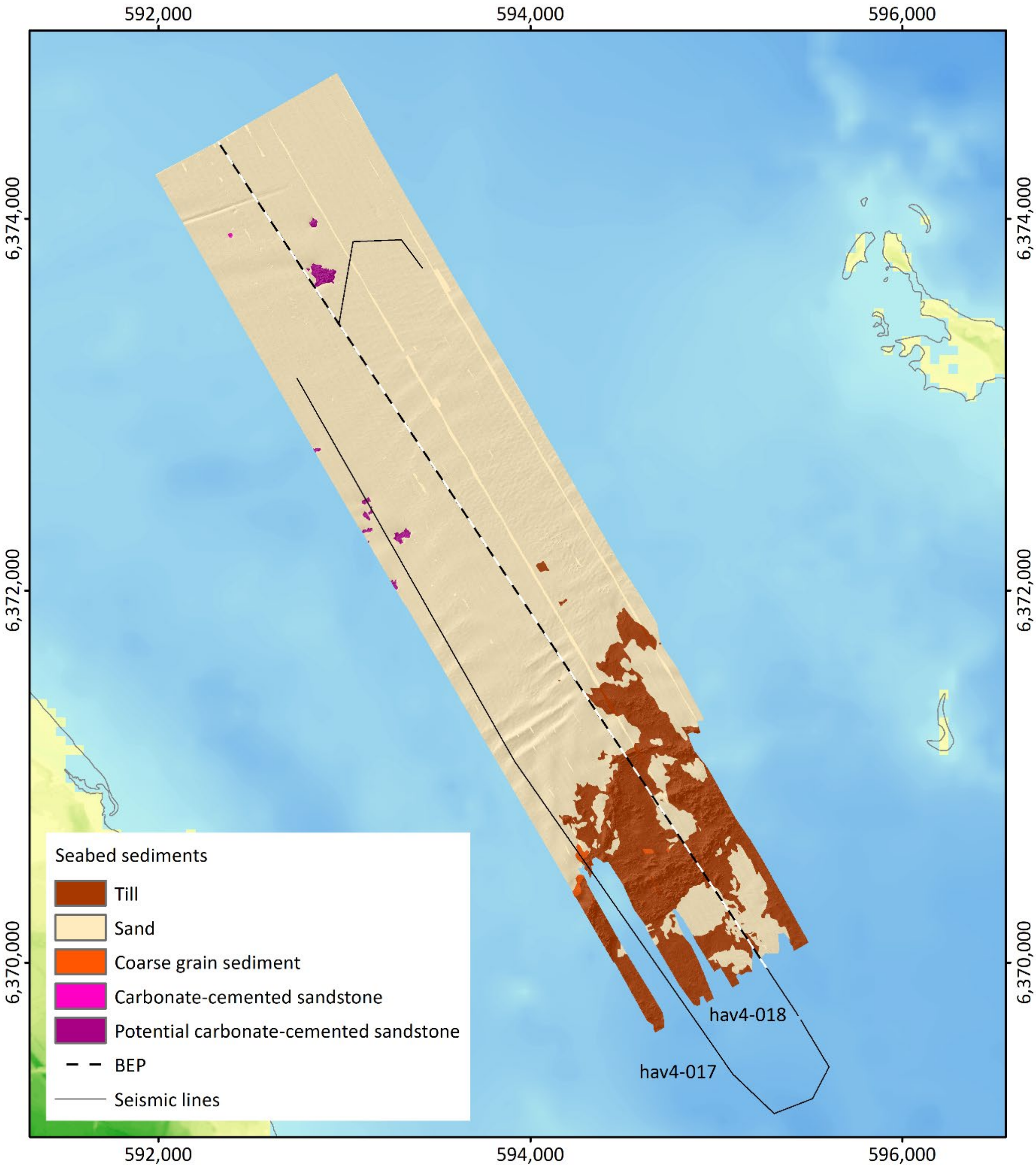

Figure 12. Seabed sediment map of the test site in the Hirsholmene marine habitat area off Frederikshavn adapted to a grid cell size of 1 m (for location see Figure 3). The seabed sediment classification serves as EG-input to the geodiversity index computation. The background is the national DEMs of topography and bathymetry available from the Danish Geodata Agency. Projection is ETRS89 UTM Zone 32N with units in meter.

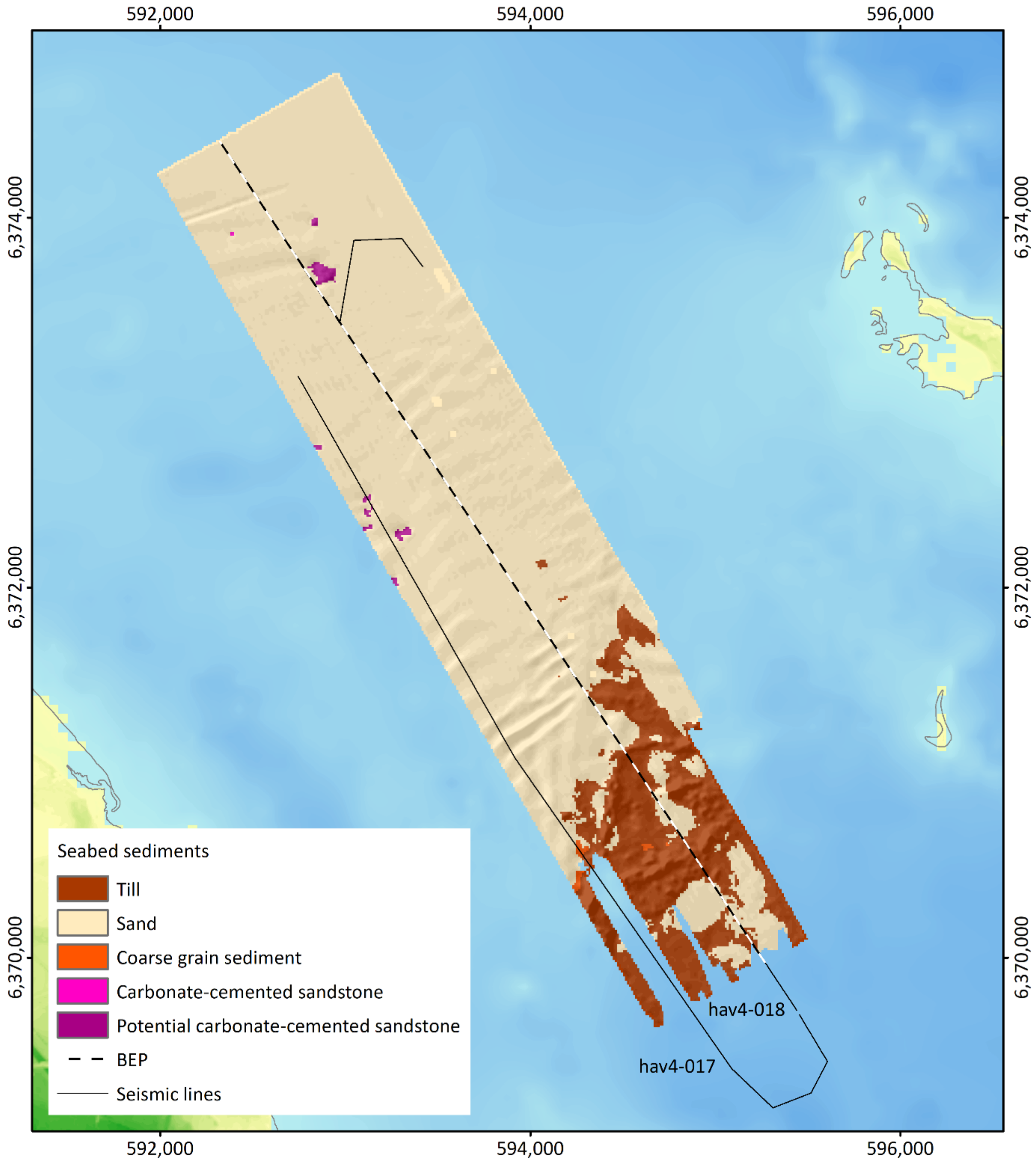

Figure 13. Seabed sediment map of the test site in the Hirsholmene marine habitat area off Frederikshavn adapted to a grid cell size of 11 m (for location see Figure 3). The seabed sediment classification serves as EG-input to the geodiversity index computation. The background is the national DEMs of topography and bathymetry available from the Danish Geodata Agency. Projection is ETRS89 UTM Zone 32N with units in meter.

The geomorphometric classification maps of the test site based on grid cell sizes of 1 m and 11 m are shown in Figure 14 and Figure 15, respectively. These are principally similar to the geomorphometric classification map shown in Figure 9.

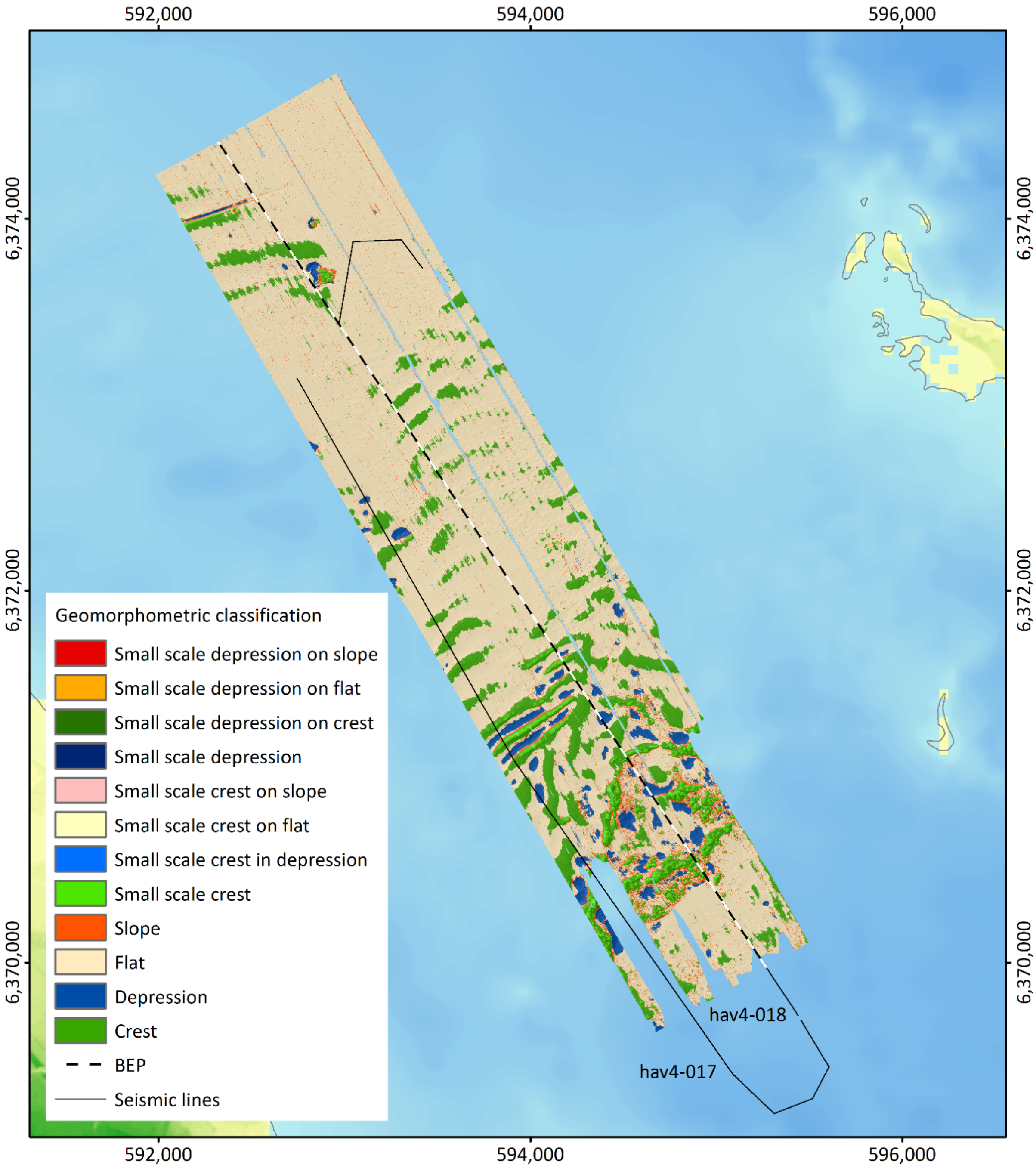

Figure 14. Geomorphometric classification map of the test site in the Hirsholmene marine habitat area off Frederikshavn based on a grid cell size of 1 m (for location see Figure 3). The geomorphometric classification serves as EG-input to the geodiversity index computation. The background is the national DEMs of topography and bathymetry available from the Danish Geodata Agency. Projection is ETRS89 UTM Zone 32N with units in meter.

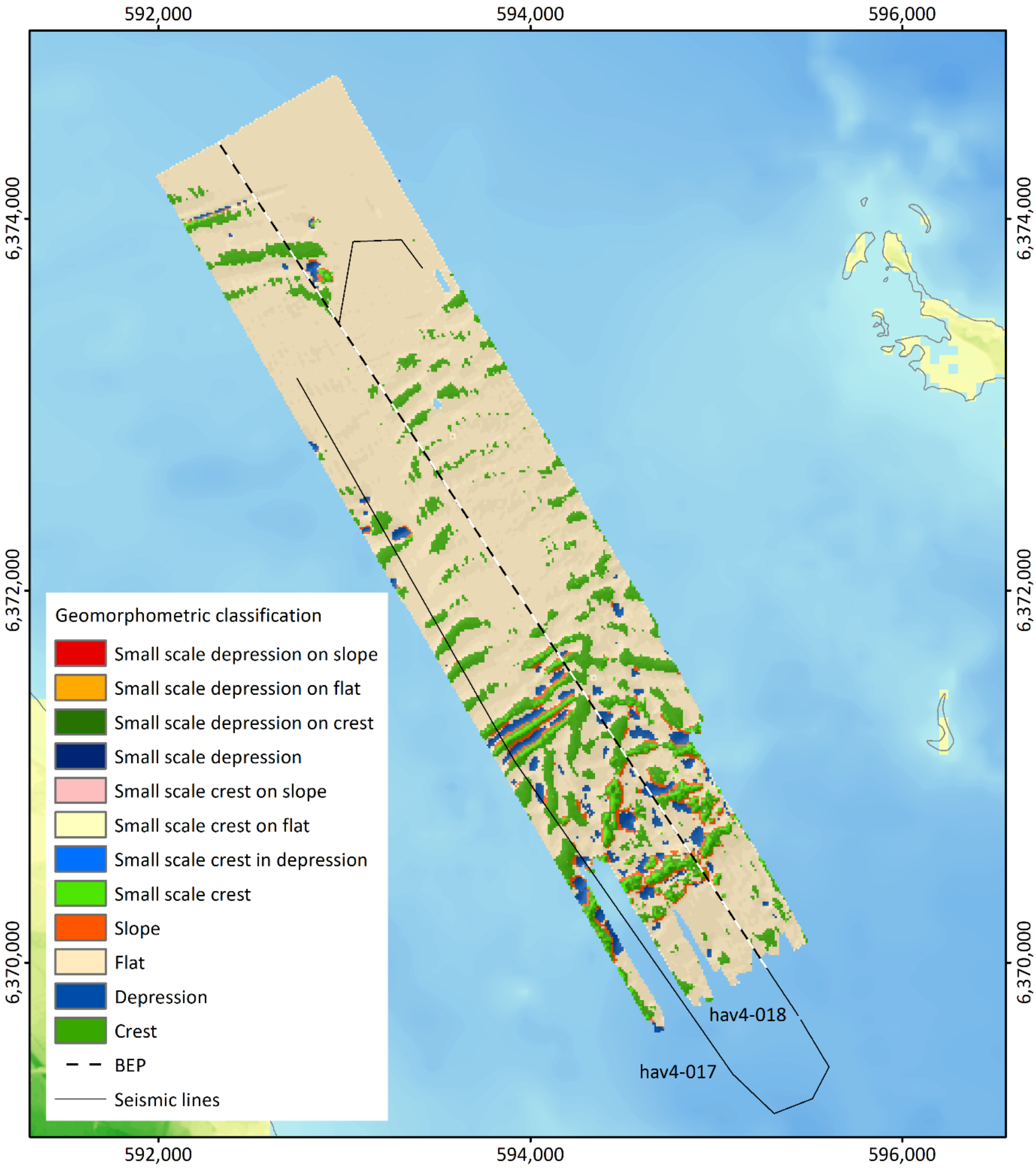

Figure 15. Geomorphometric classification map of the test site in the Hirsholmene marine habitat area off Frederikshavn based on a grid cell size of 11 m (for location see Figure 3). The geomorphometric classification serves as EG-input to the geodiversity index computation. The background is the national DEMs of topography and bathymetry available from the Danish Geodata Agency. Projection is ETRS89 UTM Zone 32N with units in meter.

The surface roughness (standard deviation of slope) maps of the test site based on grid cell sizes of 1 m and 11 m are shown in Figure 16 and Figure 17, respectively.

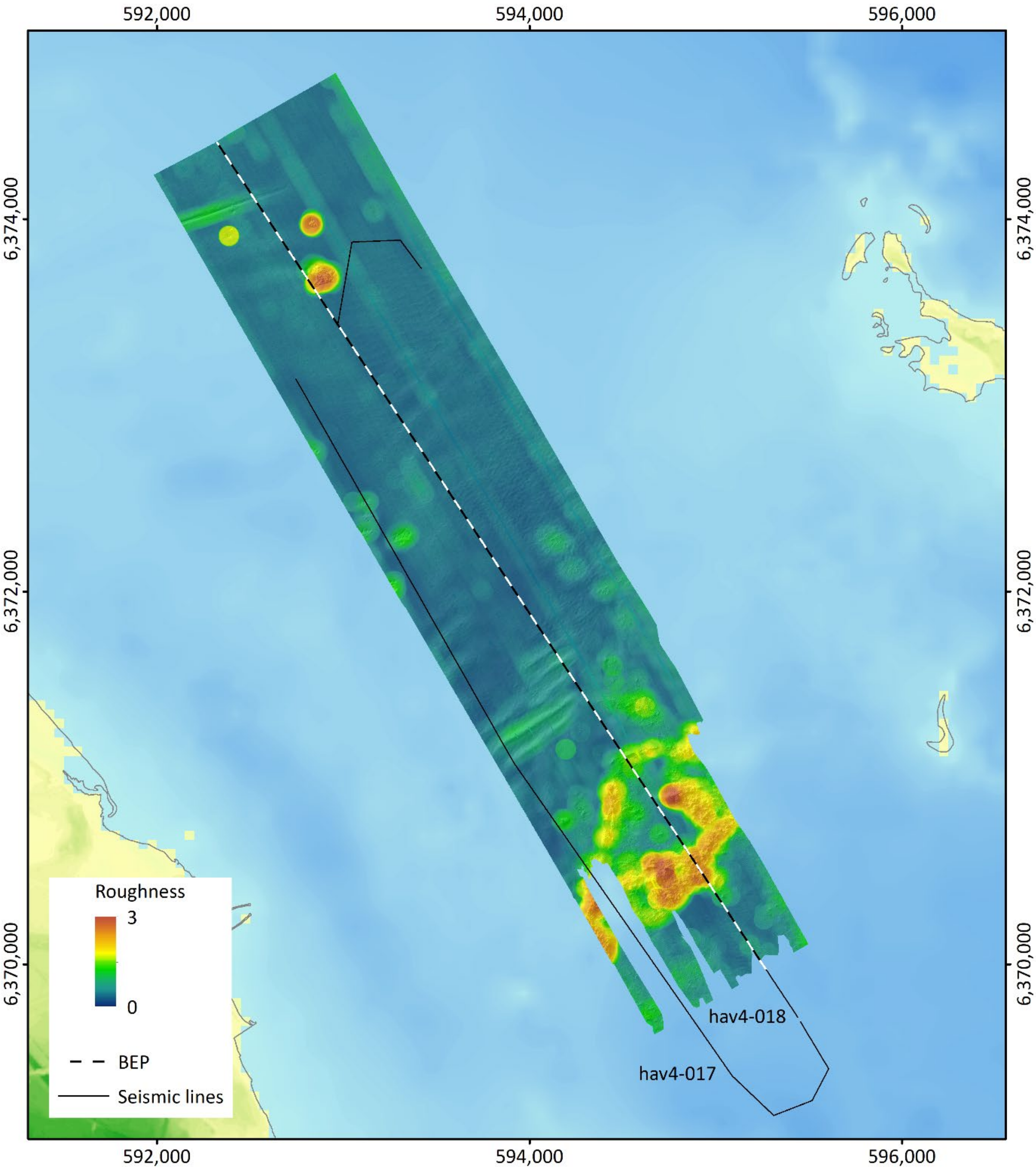

Figure 16. Surface roughness map of the test site in the Hirsholmene marine habitat area off Frederikshavn based on a grid cell size of 1 m (for location see Figure 3). The surface roughness (standard deviation of slope) serves as R-input to the geodiversity index computation. The background is the national DEMs of topography and bathymetry available from the Danish Geodata Agency. Projection is ETRS89 UTM Zone 32N with units in meter.

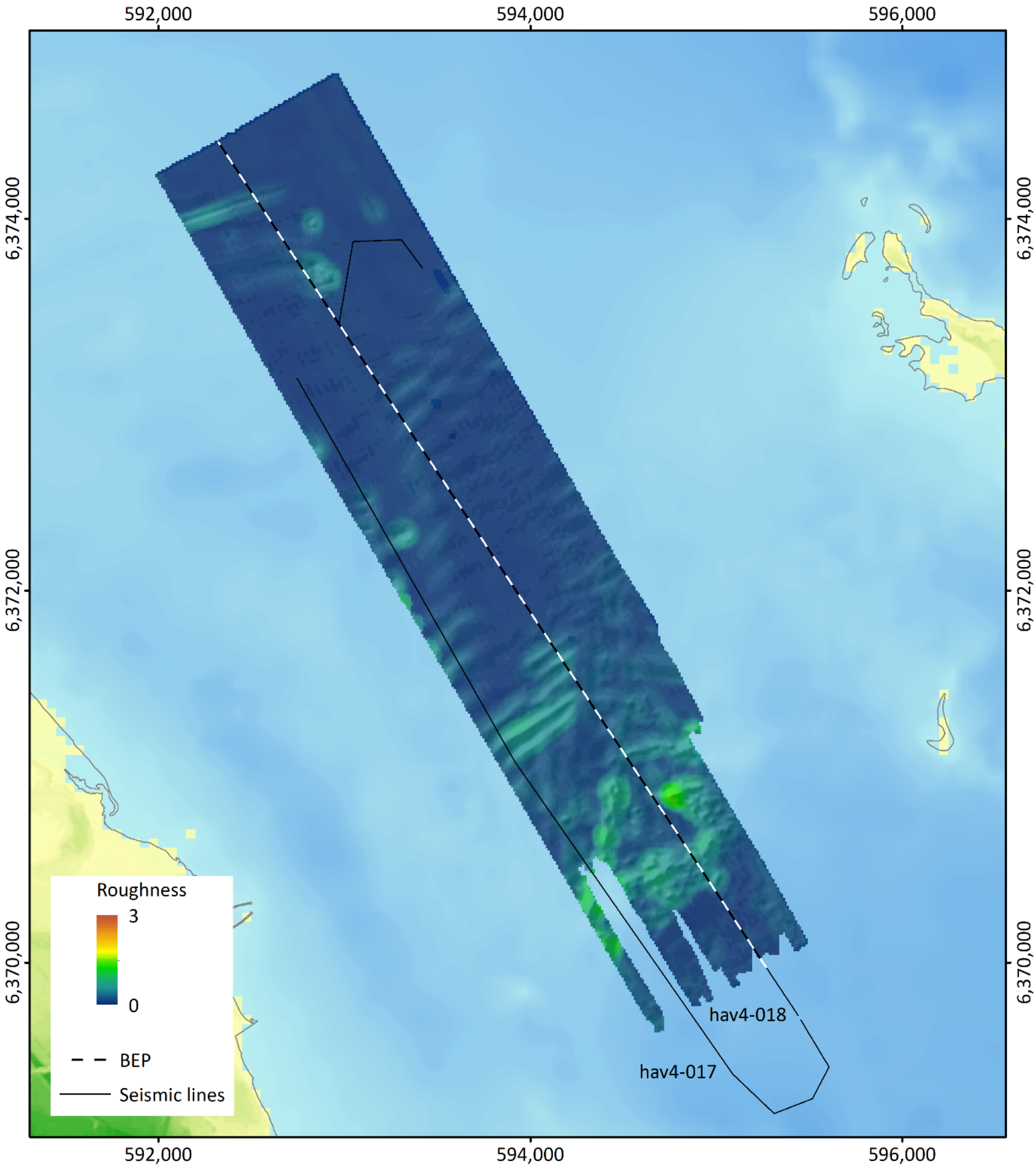

Figure 17. Surface roughness map of the test site in the Hirsholmene marine habitat area off Frederikshavn based on a grid cell size of 11 m (for location see Figure 3). The surface roughness (standard deviation of slope) serves as R-input to the geodiversity index computation. The background is the national DEMs of topography and bathymetry available from the Danish Geodata Agency. Projection is ETRS89 UTM Zone 32N with units in meter.

The geodiversity index maps computed from the seabed sediment maps (Figure 12 and Figure 13), geomorphometric classification maps (Figure 14 and Figure 15) and surface roughness maps (Figure 16 and Figure 17) of the test site based on grid cell sizes of 1 m and 11 m are shown in Figure 18 and Figure 19, respectively.

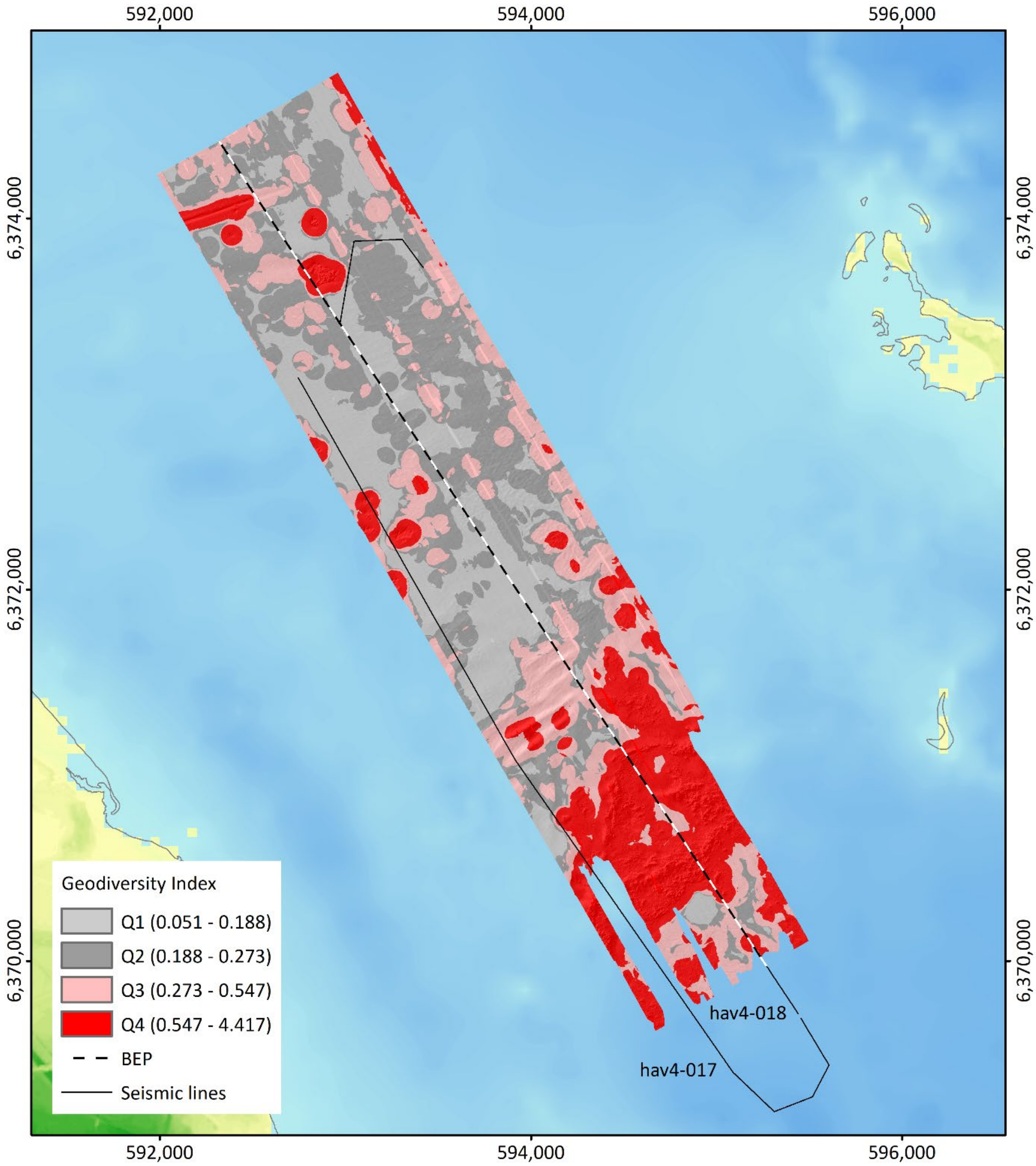

Figure 18. Geodiversity index map of the test site in the Hirsholmene marine habitat area off Frederikshavn with a grid cell size of 1 m (for location see Figure 3). The background is the national DEMs of topography and bathymetry available from the Danish Geodata Agency. Projection is ETRS89 UTM Zone 32N with units in meter.

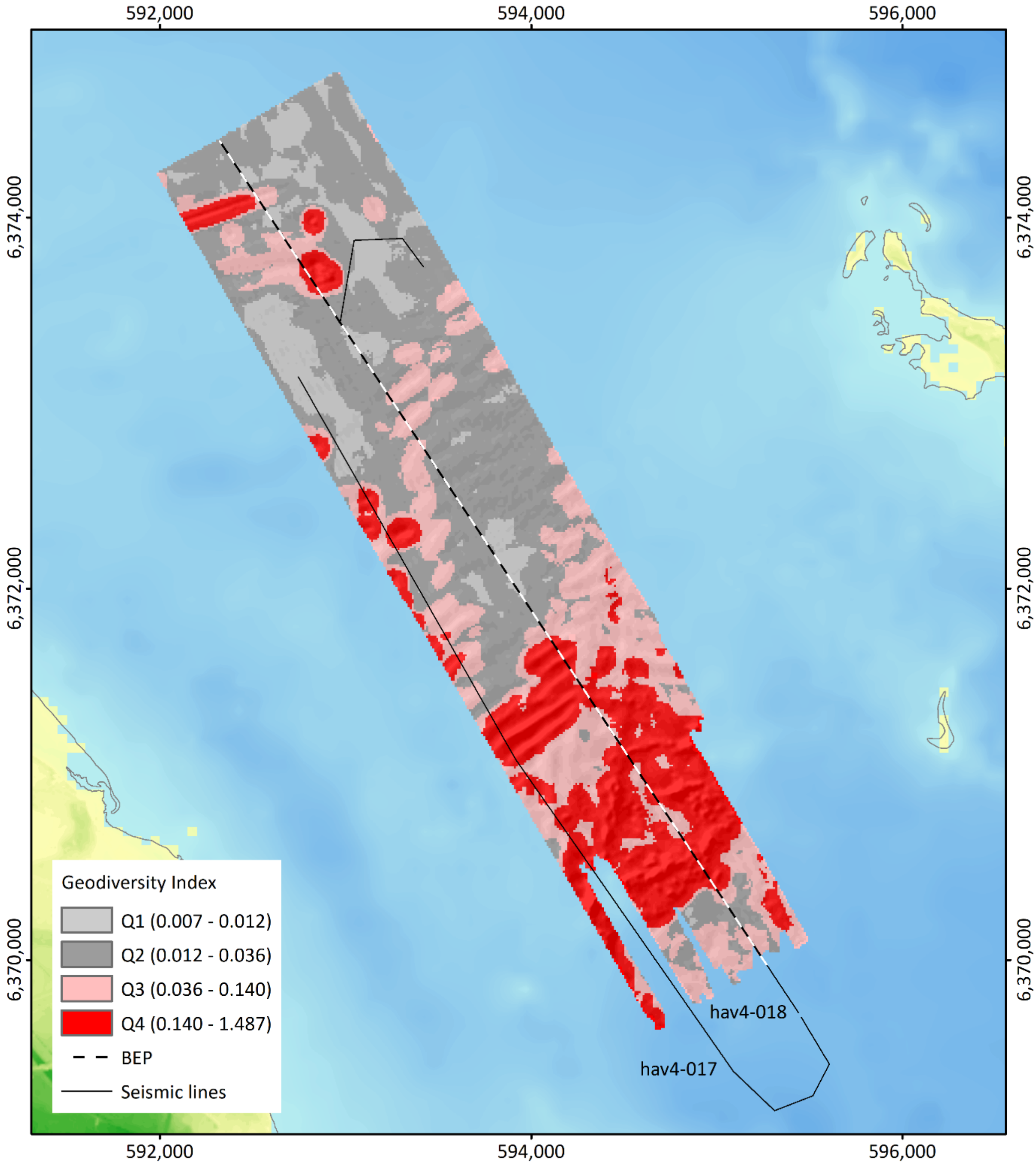

Figure 19. Geodiversity index map of the test site in the Hirsholmene marine habitat area off Frederikshavn with a grid cell size of 11 m (for location see Figure 3). The background is the national DEMs of topography and bathymetry available from the Danish Geodata Agency. Projection is ETRS89 UTM Zone 32N with units in meter.

4.6 Seabed geodiversity related to benthic habitats

We have related the spatial distribution of seabed geodiversity to the spatial distribution of specific benthic habitats at the test site in the Hirsholmene marine habitat area off Frederikshavn, i.e. we have related the spatial distribution of the geodiversity index to the spatial distribution of sandbanks, stone reefs and bubbling reefs. In general, high geodiversity index values coincide with areas classified as stone reefs and bubbling reefs, and with sandbank areas with large and distinct bedforms (see Figure 11, Figure 18 and Figure 19). More specifically, the smaller-scale (here 1 m grid cell size) high geodiversity index values coincide with the areas with stone reefs and bubbling reefs, while the larger-scale (here 11 m grid cell size) high geodiversity index values also coincide with the large and distinct bedforms in the sandbank areas.

4.7 Seamless mapping of geodiversity in the coastal zone

Figure 20 presents a larger section of the Hirsholmene marine habitat area off Frederikshavn showing the bathymetry with a grid cell size of 1 m based on airborne topobathymetric LiDAR (upper left) and the seabed sediments extracted from the national GEUS Seabed Sediment Map (upper right). Based on these inputs, Figure 20 also shows the geomorphometric classification map (middle left), the surface roughness map (middle right), and the resulting geodiversity index map (lower right), all at a grid cell size of 1 m. The example dataset still has some artefacts, these are visible primarily in the surface roughness and therefore also have an impact on the geodiversity index. The artefacts are primarily due to the refraction correction of the data, which still needs slight adjustment.

The example shown in Figure 20 is based on the spring survey-flight conducted in the beginning of the blooming season (17 April 2019) where the water column was characterised by low turbidity due to calm weather conditions and low organic matter content. This enabled LiDAR penetration depths >10 m; whereas the penetration depth was reduced to ~6 m during the midsummer survey-flight in the blooming season (21 June 2019) due to higher water column turbidity. This highlights the potential of mapping large coastal marine areas during periods of calm weather conditions and low water column turbidity, but also the limitations during periods of comparable higher water column turbidity.

The example also demonstrates the potential of extending the detailed seabed mapping into the shallow water zone (<6 m) towards the coastline and across the land-water transition zone. Full-coverage seabed mapping by vessel borne MBES in very shallow water is very time consuming and therefore also expensive, which makes it practically inapplicable for large scale coastal zone mapping in very shallow water at national level and/or Baltic Sea level.

From a future application-perspective, one of the lessons learned is that high-resolution and full-coverage seabed mapping in shallow water coastal zones (<6 m) is feasible using topobathymetric LiDAR, and it has an enormous potential for mapping and monitoring geodiversity and benthic habitats in such shallow waters (<6 m). Hence, topobathymetric LiDAR enables seamless mapping of geodiversity and habitats in the shallow water coastal zone and across the land-water transition. However, the lidar data processing time is still considerable despite optimization of the processing pipeline throughout the ECOMAP project period. Hence, further automatization of lidar data processing is still required in order to make future mapping and monitoring applications of coastal zones at national level and/or Baltic Sea level feasible.

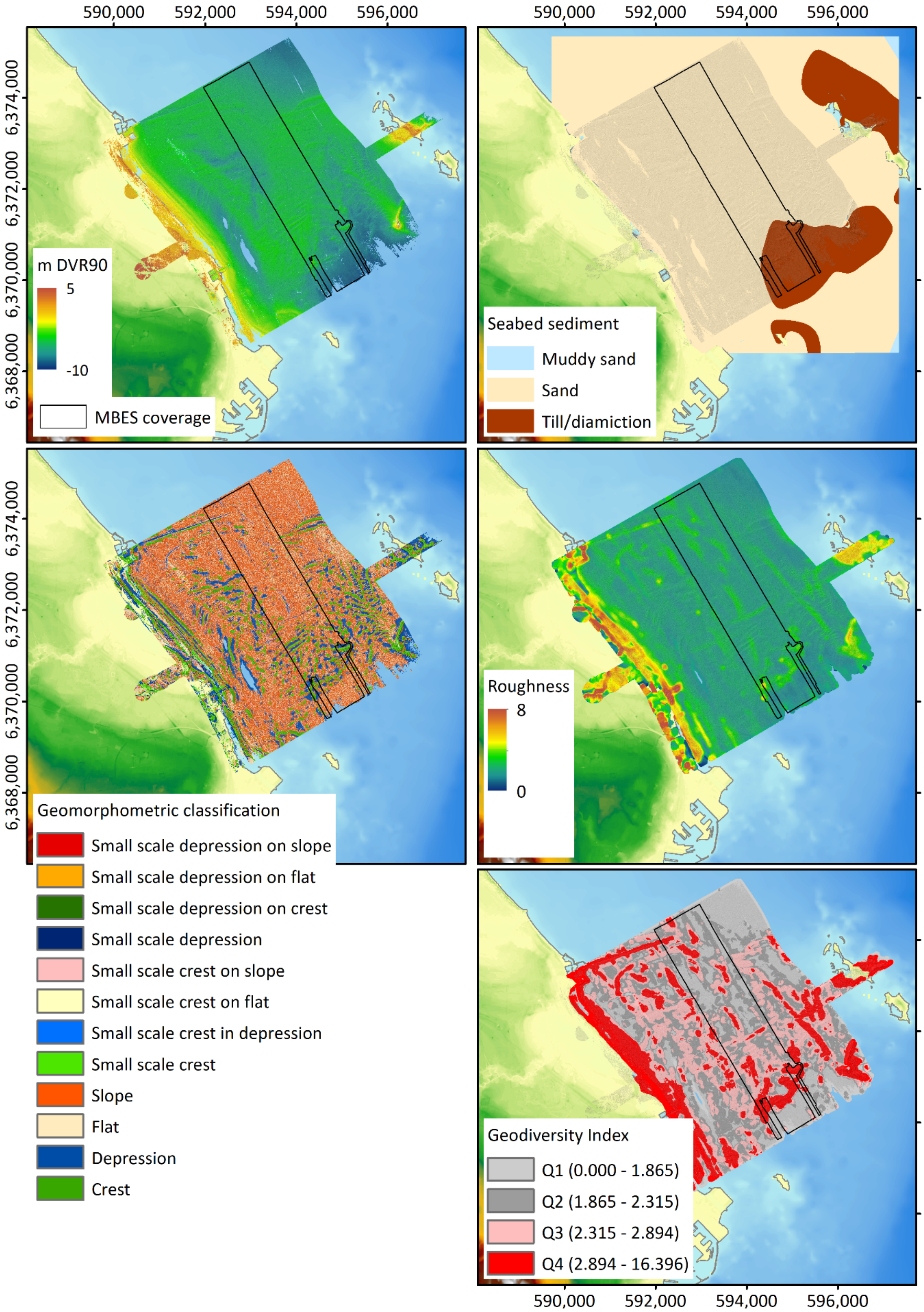

Figure 20. Upper left: Bathymetry at Hirsholmene off Frederikshavn derived from airborne topobathymetric LiDAR. The digital elevation model (DEM) is shown with a grid cell size of 1 m. Upper right: Seabed sediment map derived from the national GEUS Seabed Sediment Map and adapted to a grid cell size of 1 m. Middle left: Geomorphometric classification map based on a grid cell size of 1 m. Middle right: Surface roughness map based on a grid cell size of 1 m. Lower right: Geodiversity index map with a grid cell size of 1 m. The background is the national DEMs of topography and bathymetry available from the Danish Geodata Agency. Projection is ETRS89 UTM Zone 32N with units in meter.

5 Discussion

5.1 Developing conceptual models

The Hirsholmene marine habitat area off Frederikshavn displays the following benthic habitats: bubbling reefs, stone reefs and sandbanks, as well as seagrass meadows (generally Zostera marina or eelgrass, cf. NST (2013) and Figure 4). The role of subsurface geology and surface geomorphology for the distribution of benthic habitats at the test site is schematised in Figure 21.

The bubbling reefs are closely connected to the geological history of the area. The combination of large Quaternary deposits, which contain biogenic deposits of the Eemian interglacial, with active faulting enables the release of biogenic gases in the seabed and also at the seabed surface and into the water column. This allows the generation of bubbling reefs due to carbonate-cemented sandstone structures, where the cementation occurs in the subsurface and subsequent erosion of the surrounding unconsolidated sediment expose the reefs.

The stone reefs are the exposed glacial moraine, which may be part of the marginal moraines observed and inferred on land (cf. Figure 2).

The sandbanks with superimposed bedforms are related to a sand deposit, which is probably a near shore deposit from the previous low stand.

Finally, the seagrass meadows occupy the sandy areas that are less exposed and less dynamic, i.e. the areas absent of mobile bedforms.

Hence, geological and geomorphological mapping and the development of geological and geomorphological conceptual models are a prerequisite for benthic habitat mapping in the Hirsholmene marine habitat area off Frederikshavn, and also for evaluating and assessing benthic habitat maps of the area.

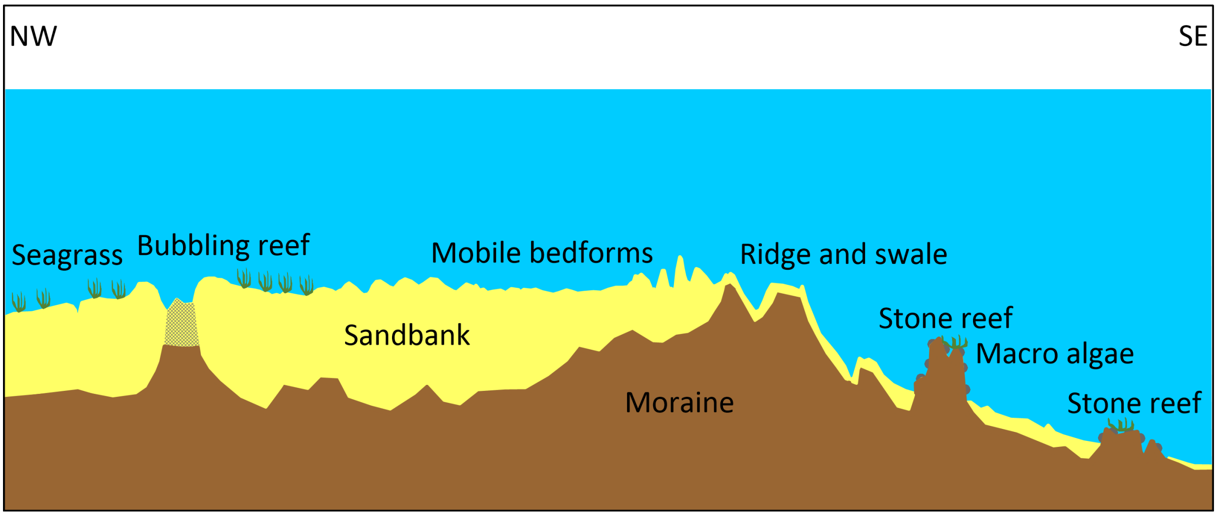

Figure 21. Schematisation of the role of subsurface geology and surface geomorphology for the distribution of benthic habitats at the test site in the Hirsholmene marine habitat area off Frederikshavn. The schematic profile conceptually illustrates the geological and geomorphological boundary conditions of the benthic habitats along the dotted line in Figure 7-Figure 19.

5.2 Mapping geodiversity

In a marine context, geodiversity encompasses the subsurface geology, the seabed sediments, and the geomorphology. In general, the geomorphology can be mapped in high detail, i.e. in high resolution and high accuracy, using e.g. vessel borne MBES or airborne LiDAR. Likewise, the seabed sediments can be mapped in relatively high detail using e.g. high-resolution side scan sonar imaging in combination with ground truth data, or by applying multifrequency MBES backscattering and MBES snippets as demonstrated in ECOMAP WP 2 and 5. It is challenging to map the subsurface geology in similar detail as the geomorphology and the seabed sediments; however, the implementation of 3D seismic/SBP imaging (in combination with coring) can decrease the gap related to 3D mapping of the subsurface geology.

The input parameters to the geodiversity index should ideally all be in high resolution and high accuracy when being applied to complex landscapes at local scale, and specifically when being applied in relation to specific habitat types such as sandbanks, stone reefs and bubbling reefs. The subsurface geology was excluded from the calculation of the geodiversity index at the test site in the Hirsholmene marine habitat area off Frederikshavn because subsurface geological layers only exist at regional scale, but not at local scale. The primary subsurface geological layers that should be included at the test site in an ideal case are e.g. the buried moraine surface, the spatial distribution of gas seepage, and the thickness of mobile sand (cf. the conceptual model schematisation in Figure 21). The buried moraine surface is important for mapping the exposure of stone reef areas, and for assessing which areas may be buried or exposed in the future due to e.g. changing sediment transport patters. The spatial distribution of gas seepage is important for mapping active bubbling reefs. The thickness of mobile sand is important for mapping the sandbank areas, and for assessing any potential increase or decrease in the areal extent due to e.g. changes in sediment erosion and deposition.

The smaller-scale (here 1 m grid cell size) high geodiversity index values coincided with the areas with stone reefs and bubbling reefs, while the larger-scale (here 11 m grid cell size) high geodiversity index values also coincided with the large and distinct bedforms in the sandbank areas. This demonstrates the potential of applying the geodiversity index at local scale for identifying and mapping valuable and relatively small-size benthic habitats. In addition, there may be a potential of using the geodiversity index as an additional quality index of benthic habitats. Hence, we recommend mapping and quantifying geodiversity as an integrated part of benthic habitat mapping.

The test case demonstrates that high-resolution, full-coverage mapping of the subsurface geology, the seabed sediments and the geomorphology is essential for improved benthic habitat mapping in compound landscape settings. It also demonstrates the need for developing conceptual geological and geomorphological models, i.e. including the processes related to the evolution and the dynamics of the seabed landscapes and the benthic habitats. This is important in order to be able to plan, evaluate and assess benthic habitat mapping and the resulting benthic habitat maps; and it is essential in relation to assessing the impacts of climate change or human impact on the dynamics of benthic habitats.

6 Summary

We have developed a catalogue for mapping geodiversity in coastal marine environments in relation to benthic habitat mapping, exemplified at the test site in the Hirsholmene marine habitat area off Frederikshavn in northern Denmark, which displays a range of key benthic habitats such as sandbanks, stone reefs and bubbling reefs.

We mapped the subsurface geology, the seabed sediments, the geomorphology, and the benthic habitats.

We integrated the seabed sediments and geomorphology in a seabed geodiversity index. The subsurface geology was excluded from the calculation of the geodiversity index at the test site because the available subsurface geological layers only exist at regional scale, but not at local scale.

We related the spatial distribution of seabed geodiversity to the spatial distribution of benthic habitats with a focus on specific habitats, including sandbanks, stone reefs and bubbling reefs.

In addition, we demonstrated that high-resolution, full-coverage mapping of the subsurface geology, the seabed sediments and the geomorphology is essential for improved benthic habitat mapping in compound landscape settings; and we demonstrated the need for developing conceptual geological and geomorphological models, i.e. including the processes related to the evolution and the dynamics of the landscape and the habitats. This is important in order to be able to plan, evaluate and assess benthic habitat mapping and the resulting benthic habitat maps; and it is essential in relation to assessing the impacts of climate change or human impact on the dynamics of benthic habitats.

Finally, we recommend mapping and quantifying geodiversity as an integrated part of benthic habitat mapping.

7 Acknowledgements

Thanks to Paul Christiansen and Per Freiberg (technicians and divers, UCPH) for assisting the ground truth data collection in the Hirsholmene area in April and June 2019.

8 References

Andersen MS, Gergely A, Al-Hamdani Z, Steinbacher F, Larsen LR, Ernstsen VB (2017). Processing and performance of topobathymetric lidar data for geomorphometric and morphological classification in a high-energy tidal environment (2017). *Hydrology and Earth System Sciences*, 21: 43-63.

Brandes C, Steffen H, Sandersen PBE, Wu P, Winsemann J (2018). Glacially induced forcing along the NW segment of the Sorgenfrei-tornquist Zone, northern Denmark: Implications for neotectonics and Lateglacial fault-bound basin formation. *Quaternary Science Reviews*, 189: 149-168.

Brilha J, Gray M, Pereira DI, Pereira P (2018). Geodiversity: An integrative review as a contribution to the sustainable management of the whole of nature. Environ Sci Policy 86:19-28.

Drăguţ L, Eisank C, Strasser T (2011). Local variance for multi-scale analysis in geomorphometry. *Geomorphology*, 130: 162-172.

Drăguţ L, Tiede D, Levick, SR (2010). ESP: a tool to estimate scale parameter for multiresolution image segmentation of remotely sensed data. *International Journal of Geographical Information Science*, 24 (6): 859-871.

EMODnet Geology (2019): https://www.emodnet-geology.eu/

EMODnet Seabed Habitats (2019): http://www.emodnet.eu/seabed-habitats

GEUS marine database MARTA: https://www.geus.dk/

Gordon JE, Brooks AJ, Chaniotis PD, James BD, Kenyon NH, Leslie AB, Long D, Rennie AF (2016). Progress in marine geoconservation in Scotland's seas: assessment of key interests and their contribution to Marine Protected Area network planning. P Geologist Assoc 127:716-737.

Gray M (2013). Geodiversity: Valuing and conserving Abiotic Nature, 2nd Edition. Wiley Blackwell, Chichester, 508 pp.

Gregersen S, Leth J, Lind G, Lykke-Andersen H (1996). Earthquake activity and its relationship with geologically recent motion in Denmark. *Tectonophysics*, 257: 265-273.

Gregersen S, Voss PH (2012). Efforts to include geological and geodetic observations in the assessment of earthquake activity in Denmark. *GEUS Bulletin*, 26: 41-44.

Hansen LØ, Ernstsen VB, Clemmensen LB, Al-Hamdani Z, Kroon A. A method for estimating sediment budgets of washover deposits using Digital Terrain Models. *Earth Surface Processes and Landforms* (submitted). *ECOMAP publication*.

Jensen JB, Petersen KS, Konradi P, Kuijpers A, Bennike O, Lemke W, Endler R (2002). Neotectonics, sea-level changes and biological evolution in the fennoscandian Border zone of the southern Kattegat Sea. *Boreas*, 31: 133-150.

Kaskela AM, Kotilainen AT (2017). Seabed geodiversity in a glaciated shelf area, the Baltic Sea. *Geomorphology*, 295: 419-435.

Kaskela AM, Kotilainen AT, Al-Hamdani Z, Leth JO, Reker J (2012). Seabed geomorphic features in a glaciated shelf of the Baltic Sea. *Estuarine, Coastal and Shelf Science,* 100: 150-161.

Krohn CF, Larsen NK, Kronborg C, Nielsen OB, Knudsen KL (2009). Litho- and chronostratigraphy of the Late Weichselian in Vendsyssel, northern Denmark, with special emphasis on tunnel-valley infill in relation to a receding ice margin. Boreas, 24 pp.

Larsen NK, Knudsen KL, Krohn CF, Kronborg C, Murray AS, Nielsen OB (2009). Late Quaternary ice sheet, lake and sea history of southwest Scandinavia – a synthesis. Boreas, 38: 732-761.

Lykke-Andersen H, Knudsen KL, Christiansen C (1993). The Quaternary of the Kattegat area, Scandinavia: A review. *Boreas*, 22: 269-281.

NST (2013). Marin habitatnaturtypekortlægning i kystnære områder 2012. Rapport udarbejdet af GEUS og Orbicon for NST, 298 pp (in Danish).

Sandersen PBE, Jørgensen F, Larsen NK, Westergaard JH, Auken E (2009). Rapid tunnel valley formation beneath the receding Late Weichselian ice sheet in Vendsyssel, Denmark. *Boreas*, 38: 834-851.

Serrano E, Ruiz-Flaño P (2007). Geodiversity: a theoretical and applied concept. *Geographica Helvetica*, 62: 140-147.

Walbridge S, Slocum N, Pobuda M, Wright DJ (2018). Unified Geomorphological Analysis Workflows with Benthic Terrain Modeler. *Geosciences*, 8, 94, 24 pp.

Weiss AD (2001). Topographic positions and landforms analysis (Map gallery poster). Proceedings of the 21st Annual ESRI User Conference. San Diego, CA.

Woodcock CE, Strahler AH (1987). The factor of scale in remote sensing. *Remote Sensing of Environment*, 21: 311-332.

Wright DJ, Lundblad ER, Larkin EM, Rinehart RW, Murphy J, Cary-Kothera L, Draganov K (2005). ArcGIS Benthic Terrain Modeler. Corvallis, Oregon: Oregon State University, Davey Jones Locker Seafloor Mapping/Marine GIS Laboratory and NOAA Coastal Services Center. Available at https://coast.noaa.gov/digitalcoast/tools/btm.